

Compound events in Germany in 2018: drivers and case studies

Elena Xoplaki^{1,2}, Florian Ellsäßer^{2,a}, Jens Grieger³, Katrin M. Nissen³, Joaquim G. Pinto⁴, Markus Augenstein⁴, Ting-Chen Chen⁴, Hendrik Feldmann⁴, Petra Friederichs⁵, Daniel Glikzman^{6,7}, Laura Goulier⁸, Karsten Hausteiner^{9,b}, Jens Heinke¹⁰, Lisa Jach¹¹, Florian Knutzen⁹, Stefan Kollet⁸, Jürg Luterbacher^{1,2}, Niklas Luther², Susanna Mohr^{4,13,12}, Christoph ~~Mudersbach~~¹⁴Mudersbach¹³, Christoph Müller¹⁰, Efi ~~Rousi~~¹⁵Rousi¹⁴, Felix ~~Simon~~¹⁴Simon¹³, Laura Suarez-~~Gutierrez~~¹⁶Gutierrez^{15,c,d}, Svenja Szemkus⁵, Sara M. Vallejo-~~Bernal~~¹⁷Bernal^{16,18,17}, Odysseas Vlachopoulos², Frederik ~~Wolf~~¹⁷Wolf¹⁶

¹ Department of Geography, Climatology, Climate Dynamics and Climate Change, Justus Liebig University Giessen, Giessen, Germany

² Centre of International Development and Environmental Research, Justus Liebig University Giessen, Giessen, Germany

³ Institute of Meteorology, Free University of Berlin, Berlin, Germany

⁴ Institute of Meteorology and Climate Research (IMK-TRO), Karlsruhe Institute of Technology (KIT), Karlsruhe, Germany

⁵ Institute of Geosciences, University of Bonn, Bonn, Germany

⁶ Institute of Hydrology and Meteorology, Faculty of Environmental Sciences, Dresden University of Technology, Tharandt, Germany

⁷ Institute of Geography, Dresden University of Technology, Dresden, Germany

⁸ Institute for Bio- and Geosciences, Research Centre Jülich, Jülich, Germany

⁹ Climate Service Center Germany (GERICS), Helmholtz-Zentrum Hereon, Hamburg, Germany

¹⁰ Potsdam Institute for Climate Impact Research (PIK), Member of the Leibniz Association, Potsdam, Germany

¹¹ Institute of Physics and Meteorology, University of Hohenheim, Stuttgart, Germany

~~¹² Science and Innovation Department, World Meteorological Organization (WMO), 7bis Avenue de la Paix, 1211 Geneva, Switzerland~~

~~^{13,12} Center for Disaster Management and Risk Reduction Technology (CEDIM), Karlsruhe Institute of Technology, Karlsruhe, Germany~~

~~^{14,3} Department of Hydraulic Engineering and Hydromechanics, Civil and Environmental Engineering, Bochum University of Applied Sciences, Bochum, Germany~~

~~^{14,5} Potsdam Institute for Climate Impact Research (PIK), Member of the Leibniz Association, Potsdam, Germany~~

~~^{15,6} Max-Planck-Institut für Meteorologie, Hamburg, Germany~~

~~^{16,7} Research Department IV - Complexity Science, Potsdam Institute for Climate Impact Research (PIK), Member of the Leibniz Association, Potsdam, Germany~~

~~^{17,8} Institute of Geosciences, University of Potsdam, Potsdam, Germany~~

^a now at: Department of Natural Resources, ITC - Faculty of Geoinformation Science and Earth Observation, University of Twente, The Netherlands

^b now at: Institute for Meteorology, University of Leipzig, Leipzig, Germany

^c now at: Institute for Atmospheric and Climate Science, ETH Zurich, Zurich, Switzerland

^d now at: Institut Pierre-Simon Laplace, CNRS, Paris, France

Correspondence to: Elena Xoplaki (elena.xoplaki@geogr.uni-giessen.de)

Abstract. ~~The European continent is regularly frequently affected experiences~~ by a wide range of extreme events and natural hazards, including heatwaves, extreme precipitation, droughts, cold spells, windstorms, and storm surges. Many of these events do not occur as single extreme events, but rather show a multivariate character, ~~the so-called known as~~ compound events. ~~Within the scope of the interdisciplinary project climXtreme (https://climxtreme.net/), we~~ We investigate the ~~interplay~~

42 ~~interactions of between~~ extreme weather events, their characteristics, ~~and~~ changes, ~~in~~ intensity, frequency, ~~as well as and~~
43 uncertainties in the past, present and future. ~~We also and explore associated their~~ impacts on various socio-economic sectors
44 in Germany and Central Europe. This contribution ~~presents highlights~~ several case studies with special ~~emphasis focus~~ on the
45 ~~calendar year of~~ 2018, which is of particular interest given the a year marked by an exceptional sequence of ~~different~~ compound
46 events across large parts of Europe, ~~resulting with devastating in severe~~ impacts on human lives, ecosystems, and infrastructure.
47 We provide ~~new insights into the new evidence on~~ drivers of spatially and temporally compound events, ~~(such as~~ heat and
48 drought ~~and;~~ heavy precipitation ~~in combination combined~~ with extreme winds), ~~and their adverse effects with adverse impacts~~
49 on ecosystems and society, using large-scale atmospheric patterns. We ~~shed light on also examine~~ the interannual influence of
50 droughts on surface water, and the impact of water scarcity and heatwaves on agriculture and forests. ~~We we assessed~~ projected
51 changes in compound events at different current and future global surface temperature levels, demonstrating the ~~importance~~
52 ~~need of for better improved quantification~~ quantifying the likelihood of future extreme events ~~for to support~~ adaptation
53 planning. Finally, we addressed research ~~needs gaps~~ and future ~~pathways directions, emphasising stressing the importance of the~~
54 ~~need to define defining~~ composite events primarily in terms of their impacts prior to their statistical characterisation.
55

56 1 Introduction

57 Extreme temperatures, strong extratropical low pressure systems and their associated extreme winds and heavy precipitation
58 events can have devastating socio-economic impacts. Moreover, the combination of otherwise regular climate and weather
59 phenomena can unfold their effects beyond the individual events (Ridder et al., 2020) and have devastating consequences ~~and~~
60 ~~impacts~~ (Ridder et al., 2022; Bevacqua et. al., 2017, 2021, 2023 and references therein). Thus, human and natural systems that
61 are usually able to handle the impacts of single extreme events are challenged by the co-occurrence of two or more extremes
62 (compound events, CE) which severely increase the risk of loss and damage (Toreti et al., 2019a). Events with additive and
63 multiplicative effects are of utmost importance and can result from mutually reinforcing cycles/positive feedbacks between
64 individual events. Interrelated events, e.g., through land surface-atmosphere interactions or atmospheric moisture conditions,
65 modify extreme events (Wang et al., 2022). The effects may develop also through atmospheric dynamics that connect features
66 such as the 2010 Russian heatwave and the flood in Pakistan (Barriopedro et al., 2011; Lau et al., 2012; Zscheischler et al.,
67 2018) or through induced responses at distant areas of significant impact to the global system (Vogel et al., 2019).
68 The Intergovernmental Panel on Climate Change (IPCC; Seneviratne et al., 2012) defines CEs as 1) two or more extreme
69 events occurring simultaneously or successively, 2) a combination of extreme events with underlying conditions that amplify
70 the impact of the events, or 3) a combination of events that are not themselves extremes but lead to an extreme event or impact
71 when combined. This definition is embedded within the IPCC risk framework under the umbrella of a combination of multiple
72 drivers and/or hazards that contribute to societal or environmental risks. Also embedded in this framework is the understanding
73 that response to an imminent risk can, in its own right, serve to reduce or to increase future risks. ~~Zscheischler et al. (2018)~~

74 ~~further defined CEs as combinations of events that are individually not necessarily extreme, or multiple drivers and/or hazards,~~
75 ~~but in combination~~ often lead to disproportionate impacts on people and ecosystems (Seneviratne et al., 2012; Leonard et al.,
76 2014; Caldeira et al., 2015; Bastos et al., 2021). To quantify the probability of CEs in today's and future climate is of great
77 importance specifically for adaptation planning for various sectors including agriculture, fisheries, river transport, energy
78 supply, tourism, etc. (Zscheischler and Fischer, 2020). Recently, Zscheischler et al. (2020) extended the definition and
79 classified CEs into 1) preconditioned events, where a weather-driven or climate-driven precondition aggravates the impacts of
80 a climatic impact-driver; 2) multivariate events, where multiple drivers and/or climatic impact-drivers lead to an impact; 3)
81 temporally compounding events, where a succession of hazards leads to an impact; and 4) spatially compounding events,
82 where hazards in multiple connected locations cause an aggregated impact. Drivers include processes, variables, and
83 phenomena in the climate and weather domain that may span over multiple spatial and temporal scales (Zscheischler et al.,
84 2020). Current research on weather and climate impacts, risks and damages often underestimates the influence of CEs (Ridder
85 et al., 2021). ~~and thus~~ It is therefore essential to adapt research strategies and tools, such as (e.g., models,) to
86 ~~incorporate~~ integrate it is essential to adapt models, processes and studies for research to incorporate compound weather and
87 climate ~~events-extremes-, enabling a more accurate assessment of in order to determine~~ uncertainties, impacts and risks.
88 Further, anthropogenic climate change is expected to influence the frequency and intensity of CEs, and thus future planning
89 for such changes requires reliable climate models, which ~~are able to~~ can represent these hazards, their underlying drivers
90 as well as their combinations. Despite this importance, studies evaluating climate model representation of CEs are still rare
91 (Aalbers et al., 2013; Bevacqua et al., 2023; Manning et al., 2023). Further, the impact of climate change to dynamic changes
92 in the atmosphere and consequently to the location and magnitude of extreme events and its compounds is less well understood
93 and thus characterised as low confidence by the IPCC (IPCC, 2021). This holds true also for CEs, ~~which~~ that are naturally even
94 more complex due to their ~~multivariate~~ multi-variate character, also in terms of the complexity of the atmospheric circulation
95 state. For instance, the COVID-19 pandemic has brought dynamics of compound hazards and risk-response ~~feedback~~ feedbacks
96 to the forefront of hydrometeorological hazard response and preparedness (Simpson et al., 2021; Zaitchik et al., 2022).
97 Compound hazards are rare, and those for instance that involve a disease such as COVID-19 have no recent precedent. The
98 more complex CEs become, the clearer are the limitations of the conventional statistical approaches to risk assessment (Zaitchik
99 et al., 2022).

100 The development of integrated research on CEs is the objective of the European COST Action DAMOCLES
101 (<http://www.damocles.compoundevents.org>) that bundled research efforts in this field, and towards which several of the
102 authors actively contribute. One of the main knowledge gaps identified concerns how the compound character of events is
103 changing in a warming ~~world, and~~ world and will continue to change during future decades. The question on how and why
104 extreme weather events affecting specifically Germany and Central Europe may change in a warming climate is the major
105 topic of the climXtreme project (<https://climxtreme.net/>), ~~in the frame of which this work has been conducted, aiming to~~
106 analyze and understand the dynamics of extreme climate events, their impacts, and potential future trends in a changing climate.
107 ~~climXtreme is funded by the German Federal Ministry of Education and Research (BMBF) and comprises 35 universities and~~

108 ~~research institutions from all over Germany. The project's vision is to address some of the topics and challenges described~~
109 ~~above providing new evidence and answers to questions whether extreme events and CEs are already occurring more frequently~~
110 ~~as a result of climate change, and how anthropogenic climate change will alter the intensity, frequency and spatial distribution~~
111 ~~of extreme and CE events in the future. A group within climXtreme joined forces to analyse CEs of temperature and~~
112 ~~precipitation as well as of precipitation and wind.~~ To analyse hot and dry compounds, a variety of research questions and
113 approaches are explored: at the global scale, the precursors of spatially and temporally CEs are analysed using large-scale
114 atmospheric patterns and jet stream states. At the European scale, the detection and identification of events and the spatial
115 representation of key climate variables in relation to heatwaves are investigated. Focusing on Germany, the interannual
116 influence of droughts on surface water is analysed and the impact of water scarcity and heatwaves on agriculture and forests
117 is studied. Further, the CEs including precipitation and/or wind as a hazard are analysed focusing on a series of windstorms
118 and convective storms with adverse impacts on ecosystems and society.

119 All case studies presented in this paper are selected from the calendar year 2018, which is of particular interest given the
120 prolonged and persistent dry and hot conditions across large parts of Europe as well as featured storms Eleanor and David
121 (coined Burglind and Friederike in Germany and hereafter) in January 2018 and several weeks of thunderstorm activity in May
122 and June. 2018 was also characterized by strong wind gusts that co-occurred with heavy snowfall during the windstorm
123 Friederike (Vautard et al., 2019), a relatively dry spring with exceptionally high temperatures followed by an extremely dry
124 summer with very warm mean temperatures over large areas of Europe (Munich Re, 2019; ~~Toreti et al., 2019a~~; Zscheischler
125 and Fischer, 2020). Total precipitation in central Europe was at the lowest percentiles relative to the 1976–2005 distribution;
126 Germany experienced a reduction of precipitation of ~~~42~~53% in July and of ~~45~46~~% in August compared to the period 1981-
127 2010 (Deutscher Wetterdienst, 2018; Toreti et al., 2019a,b). The summer in Germany was characterised by the most extreme
128 combination of high temperatures, as one of the warmest years on record (Kaspar et al., 2023); and low precipitation since
129 1881 (Zscheischler and Fischer, 2020). The combination of the individual events caused tremendous adverse and detrimental
130 impacts in larger areas of western Europe with a peak over Germany and on a variety of sectors ranging from agriculture and
131 society (Manning et al., 2018; Toreti et al., 2019b; Zscheischler and Fischer, 2020; Conradt et al., 2023; Shyrokaya et al.,
132 2024), forests (Bastos et al., 2020; Buras et al., 2020; de Brito et al., 2020; Senf and Seidl, 2021), fires (Munich Re 2019;
133 Bastos et al., 2020), ecology (Bastos et al., 2021), soil and surface water (Liu et al., 2020; Brakkee et al., 2022; Hartick et al.,
134 2021), marine environment (Kaiser et al., 2023), traffic disruption, power outages, property damage by e.g. falling trees,
135 fatalities (Vautard et al., 2019) as well as human health (Matzarakis et al., 2020; Conradt et al., 2023). The exceptional
136 heatwave of 2018 also caused many nuclear power plants to shut down because the rivers could not provide sufficient cooling
137 capacity for the reactors~~the warm water in the rivers could not adequately cool the reactors~~ (Vogel et al., 2019). In addition,
138 Blauhut et al. (2022) surveyed stakeholders across Europe regarding their perceptions of the 2018–2019 drought and drought
139 risk management in their respective countries. Germany was identified as being aware of drought risks but among the least
140 prepared, lacking a formal management plan.

141 We study this exceptional year and the series of extremes and CEs in a sequence of the large scale, their detection and spatial
142 representation as well as the long term impacts on soil moisture both at the continental scale and the consequent agriculture
143 and forestry impacts at the national scale. The paper first outlines the data and methodologies used for analysing the selected
144 CEs in 2018, followed by a detailed analysis of each case study. These case studies are categorized into temperature-
145 precipitation and precipitation-wind CE storylines, along with an evaluation of their impacts in Germany~~The paper presents~~
146 ~~first the different data used and methodologies applied for the analysis of the selected CEs during 2018 followed by analyses~~
147 ~~of each case study. The case studies are clustered in temperature-precipitation and precipitation-wind CE storylines together~~
148 ~~with an assessment of their impacts in Germany.~~

149 **2 Data and Methods**

150 Different methodological approaches have been used~~employed~~ The sub projects of climXtreme employ different
151 methodological approaches, tailored to the different types of CEs-addressed, corresponding research questions ranging from
152 better understanding of the selected event~~events~~ drivers to sectoral impact assessments. This section summarizes these
153 approaches and provides a basis for the study and analysis of the selected case studies separated in temperature-precipitation
154 and precipitation-wind CEs. The temperature-precipitation storyline includes analysis on drivers of the hot summer of 2018,
155 detection of extreme events and spatial patterns, assessment of the impact of the 2018 European drought on soil moisture and
156 groundwater as well as sectoral impacts on agriculture and forestry. The storyline is complemented with an assessment of
157 model simulations to realistically represent conditions as those of 2018 in Germany. The precipitation-wind storyline
158 comprises the analysis of intense low pressure systems in winter 2018, their life cycle and triggering role for compound
159 precipitation and wind events, as well as severe convective storms during the 2018 warm season. Considering the nature of the
160 various case studies and events during the warm season of 2018, and given the focus on compound events in this study, we
161 aim to define the characteristics of the events analysed and their interrelationships. Additionally, a range of relative thresholds,
162 such as the 90th, 95th, and 98th percentiles, appropriate for each variable and elaborated impact are used to define extremes,
163 and we will provide explanations for their application.

165 **2.1 Drivers of the hot summer of 2018**

166 To better understand the drivers of the hot summer of 2018, Rousi et al. (2022) identified jet states in the zonal mean zonal
167 wind over the Eurasian sector at different pressure levels for the summer months in ERA5 data (Hersbach et al., 2020) using
168 Self-Organizing Maps (SOMs, see Kohonen, 2013; Rousi et al., 2015). A comparative approach with different cluster numbers,
169 clustering algorithms and initializations of SOMs led to a robust cluster of double jet states. Increased persistence of those jet
170 states was connected to heatwave events (defined as a period of at least 3 consecutive days of daily maximum temperature

171 threshold exceedance > 90th percentile, following Fischer and Schär (2010) and a spatial extent over 40.000 km² within a 4°
172 x 4° spatial sliding window, similar to Stefanon et al. (2012) across western Europe (Rousi et al., 2022).

173 2.2 Detection of spatial patterns of extreme events

174 The analysis of the large-scale temperature and precipitation deficit patterns and their expression during the 2018 heatwave at
175 the European scale is based on the cross-Tail Pairwise Dependence Matrix (cross-TPDM) and Extreme Pattern Index (EPI)
176 proposed by Szemkus and Friederichs (2024). ~~The TPDM can be considered as an analogue of the covariance matrix for~~
177 ~~extremes (Cooley and Thibaud, 2019).~~ Typical spatial patterns of common extremes are derived by singular value
178 decomposition of the cross-TPDM. The cross-TPDM is a measurement of extremal dependence, rooted in extreme value theory
179 and has comparable statistical properties to the cross-covariance matrix (Szemkus and Friederichs, 2024; Cooley and Thibaud,
180 2019). The singular vectors of cross-TPDM represent pairs of spatial patterns in which extremes in two variables are likely to
181 occur simultaneously. Consequently, the expansion coefficients provide a time series for each singular vector that summarise
182 the occurrence of extreme events within the respective pattern. The first 10 left and right expansion coefficients are then
183 summarised in the EPI that is high when individual patterns or a linear combination of leading patterns are particularly strongly
184 pronounced. This pattern-based analysis thus provides a robust measurement for the heatwave and drought intensity over
185 Europe. Before calculating the cross-TPDM and EPI, the ERA5 daily 2m temperature and precipitation deficits for the summer
186 months (June-August) of 2018 are standardised and the annual cycle is removed. Precipitation deficits are calculated as the
187 inverse of the 90-day accumulated precipitation. ~~A singular value decomposition is performed on the cross-TPDM, the singular~~
188 ~~vectors are analysed and the EPI is calculated from the first 10 left and right expansion coefficients.~~

189 2.3 Surface water storage of the dry summer of 2018

190 To analyse the drought characteristics of the summer of 2018, an ensemble of simulations for the hydrological year 2018/19
191 is used (Hartick et al., 2021). The hydrological year 2018/2019 was initialised with land surface and subsurface conditions
192 from the end of the hydrological year 2018, and simulated using different atmospheric boundary conditions. The proposed
193 approach investigates the impact of hydrologic initialization, and soil and groundwater memory on water storage anomalies
194 against the background of atmospheric variability and uncertainty on an interannual time scale. The varying atmospheric
195 initialise conditions were derived from the each individual year of ERA-Interim5 data for each individual year of as
196 climatological time series between 1996 and 2018 and. This approach resulted in 22 realisations as the number of individual
197 years within that period. Thus, the ensemble of 22 realisations of the hydrological year 2018/2019 ~~as such~~ accounts for a large
198 part of the atmospheric uncertainty. The analysis was performed for 20 European river basins. The 2018 drought was defined
199 as the driest 10% of the total water storage anomalies (S) occurring in 2018 within the climatological time series. Surface water
200 availability for the 2018/2019 hydrological year was represented by surface water storage (S_u), categorised into dry, $S_{u,d}$, and
201 wet, $S_{u,w}$, anomalies. To ensure that an increased probability of $S_{u,d}$ in the hydrological year 2018/2019 was outside of regular
202 climate variability, we compared the $S_{u,d}$ probability distribution of the described hydrological year 2018/2019 ensemble (Case

203 A) with the probability distribution of $S_{u,d}$ within the climatological time series (Case B), see also the corresponding section
204 below. Two beta distributions were generated, one for each case, by applying a prior with no information. We sampled each
205 beta distribution 10,000 times and calculated the probability ~~of that~~ Case A > Case B to determine the confidence that the
206 probability of a $S_{u,d}$ after a drought is greater than the climatological variability. In addition, we obtained the uncertainty of the
207 confidence intervals by bootstrapping 1000 times over the climatological time series. The methodology provides a probabilistic
208 insight into the impact of a groundwater drought on future surface water resources on an interannual time scale.

209 **2.4 Soil moisture of the dry summer of 2018**

210 In addition to the dry surface water anomaly in Central Europe, soils showed moisture deficits (Liu et al., 2020; Bastos et al.,
211 2020; Rousi et al., 2023; [Conradt et al., 2023](#)). This likely caused low groundwater levels (Brauns et al., 2020; [Conradt et al.,](#)
212 [2023](#)), as infiltration of precipitation water is considered to be the most important groundwater source in Central Europe
213 (Brakkee et al., 2022). ERA5 soil moisture was evaluated for the four soil layers over the period 2018-2020 and compared
214 against the climatology averaged over 1991-2020 in order to assess the strength of the soil moisture deficit and its persistence
215 during the consecutive drought years 2018-2020. For this analysis, time series of daily means as well as centred 92-day running
216 means were computed for all land points of the study area 4° - 16° E and 45° - 55° N, covering Germany and adjacent regions.
217 The evaluation of soil moisture in the lowest soil layer also gives an indication of the groundwater reservoir as it interacts with
218 the aquifer in the modelling system (Cerlini et al., 2021).

219 **2.5 Agricultural and hydrological drought of the year 2018**

220 Lack of sufficient soil moisture, resulting from shortage of precipitation and excess evapotranspiration leads to agricultural
221 drought. Lack of run-off and surface water result in hydrological drought (streamflow deficits) (Seneviratne et al., 2021). To
222 estimate the severity of agricultural and hydrological droughts across Europe during summer 2018, we employed the nitrogen
223 version of the vegetation, crop, and hydrology model LPJmL (Schaphoff, et al., 2018; von Bloh et al., 2018; Lutz et al., 2019;
224 Herzfeld et al., 2021). The analysis is based on 69 years (1951-2019) obtained from model simulations driven with daily
225 temperature, precipitation, and radiation data from the GSWP-W5E5 dataset (Kim, 2017; Cucchi et al., 2020; Lange et al.,
226 2022) at 0.5 arc-degree resolution. To assess agricultural drought, the evapotranspiration deficit calculated as the ratio of actual
227 evapotranspiration to potential evapotranspiration (ET/PET ratio) over the growing season of maize in each year is determined
228 and a generalised beta distribution (a three-parameter probability distribution for variables in a bounded interval) is fitted to
229 the 69 annual values in each grid cell. An ET/PET ratio of less than 1 indicates water deficit or water stress. For the assessment
230 of the hydrological drought, the average river discharge (Dis) during the summer months (June, July, and August) of each year
231 is determined and a generalized gamma distribution (a three-parameter probability distribution for non-negative variables) is
232 fitted to the 69 annual values in each grid cell. Using the fitted distributions, the return period of the conditions in 2018 is
233 determined. To support comparability with other drought indices such as the Standardized Precipitation Evapotranspiration
234 Index (SPEI), the drought severity is also calculated, which is the probability (inverse of return period) of a given year

expressed as its distance from the mean (in number of standard deviations) in a standard normal distribution (McKee et al., 1993; Vicente-Serrano et al., 2010). For example, a return period of 44 years is equivalent to the 2.28th percentile, which is -2 standard deviations away from the mean and would be assigned a drought severity of -2.

2.6 Impact on the agricultural production of 2018

In comparison with the past three decades, the year 2018 was identified as a year with severe winter wheat yield losses estimated using a compilation of LOESS (locally estimated scatterplot smoothing; to take into account improvement of agricultural practises (Zampieri et al., 2017)) detrended and gap-filled yield data at county level aggregated from a variety of sources including the Regionaldatenbank Deutschland (Statistische Ämter des Bundes und der Länder, 2021) and the Statistical Offices of the federal states of Germany (Ellsäßer and Xoplaki 2022abc; Ellsäßer and Xoplaki, 2023,2024). The resulting annual gridded yield data was evaluated using the Standardized Yield Anomaly Index (SYAI) that expresses yield anomalies in terms of standard deviation from a 30-year time series. The analysis is based on the ~~heat stress index~~ Heat Magnitude Index (HMD) (Zampieri et al., 2017), the drought index SPEI (Vicente-Serrano et al., 2010) and the Combined Stress Index (CSI) (Zampieri et al., 2017) that accounts for stress compounds of heat and drought through a (ridge-regression based) superimposition of HMD and SPEI, using the temperature and precipitation series from E-OBS (Cornes et al., 2018). In order to derive crop relevant results, all indices were evaluated for the most vulnerable stages of phenological crop development according to the specific region using the German Weather Service (DWD) phenological data set (Kaspar et al., 2015). A spatially explicit linear regression between yield anomaly and stress indices was computed for time series covering the past three decades and the coefficient of determination (R^2) was calculated to express the proportion of yield anomaly that can be explained by heat, drought or compound stress.

2.7 Loss and damage of compound vs. non-compound wind extreme events of the winter 2018

The precipitation-wind storyline starts with a description of the synoptic situation during the winter season 2018. The cyclone track analysis in this section is based for the 2018 winter season is based on the cyclone tracking methodology of Murray and Simmonds (1991) and Pinto et al. (2005) applied to ERA5 data (Hersbach et al., 2020).

~~In the context of the UN Framework Convention on Climate Change (UNFCCC) process, L~~oss and damage ~~in this section is defined according to the UN Framework Convention on Climate Change (UNFCCC) as~~ the harm caused by anthropogenic (human-generated) climate change (UNFCCC, 2021; OECD, 2021 and references therein). ~~For the quantitative assessment of the impact of compound events (CEs) in terms of loss and damage, a compound wind and precipitation extreme is defined when both variables exceed their local 98th percentile (Martius et al., 2016). For winter events, these percentiles are calculated using data from the December to February season. Co-occurrence is defined when wind gusts and precipitation both exceed their respective 98th percentile at a specific grid box, with precipitation exceedance occurring on the same day, the day before, or the day after, within a 50 km radius around the grid box centre.~~

267 For the quantitative assessment of the impact of CEs in terms of loss and damage, a compound wind and precipitation extreme
268 is defined when the local 98th percentile of both variables is exceeded (Martius et al., 2016). For winter events, the calculation
269 of the percentile is based on data from the December to February season. The co-occurrence should be on the same day or the
270 following day for precipitation, in the same grid cell and within a radius of 50 km, respectively. The daily loss data for
271 residential buildings accumulated over Germany provided by the German Insurance Association (GDV) are categorised by
272 days on which a CE occurred and days on which it did not. This results in two separate loss distributions for compound and
273 non-compound events. ~~The cyclone track analysis for the 2018 winter season is based on the cyclone tracking methodology of~~
274 ~~Murray and Simmonds (1991) and Pinto et al. (2005) applied to ERA5 data (Hersbach et al., 2020).~~
275

276 **2.8 Concurrent heavy rain and storm extremes – estimation of probability of event occurrence**

277 The estimation of the probability of occurrence of compound heavy rain and wind is carried out on precipitation and wind time
278 series from DWD weather stations. Multivariate distributions in the form of copulas are used to determine the probability of
279 occurrence of combined events. Copulas make it possible to model the dependency structure of the variables under
280 consideration independently of their marginal distributions (e.g. Manning et al., 2024 and references therein). This allows for
281 the use of any distribution function for the marginal distributions. This means that any distribution function can be used for
282 the marginal distributions.

283 ~~We carried out fitting tests are carried out for both the marginal distributions and the copulas. However, Archimedean copulas~~
284 ~~are generally preferred when dealing with hydrological parameters. However, there is a preference for the use of Archimedean~~
285 ~~copulas in the context of hydrological parameters (Bender, 2015; Jane et al., 2020). In this particular case instance, the Frank~~
286 ~~copula (Frank, 1979) was chosen as the most appropriate option (Frank, 1979). Archimedean copula functions are used, in~~
287 ~~particular the Frank copula (Frank, 1979).~~ The Frank copula is a one-parametric copula in which the copula parameter *theta*
288 can be determined from the correlation between random variables. The approach treats the extremes of the two variables (rain
289 and wind) separately. The annual maximum values (AMAX) are extracted from the time series and tested for statistically
290 significant trends using the Mann-Kendall test at a 5% significance level. ~~In this context, Sstationary methods of extreme~~
291 ~~value statistics are applied, thus requiring the assumption of independence and identical distribution (i.i.d.) of all time series.~~
292 ~~Consequently, series with significant trends are homogenised using linear regression. If significant trends are found, the time~~
293 ~~series are homogenised using a linear regression model.~~ The distribution parameters of the strong wind and precipitation data
294 sets are then determined using maximum likelihood. In addition, the correlation between heavy rain and storm is calculated
295 using the Kendall rank correlation. For each AMAX wind value, the concurrent precipitation value is selected and vice versa.
296 To ensure the independence of precipitation events, wet episodes are separated by a dry period of at least as long as the
297 accumulation period. Due to this restriction, not all AMAX wind events can be paired with a precipitation episode, even when
298 precipitation is present, e.g., for longer precipitation durations (>1day) and considering a ± 2 -day window, no AMAX wind
299 and precipitation episode pairs exist. Subsequently, these pairs of values are applied to adjust the marginal distributions and
300 copulas, thereby determining the combined probabilities of occurrence.

301 2.9 Rockfall events

302 Rockfall is an impact that can be triggered by extreme precipitation (e.g., Nissen et al., 2022). Favourable preconditions, such
303 as previous freeze-thaw cycles and enhanced sub-surface moisture, increase the susceptibility for such events. A logistic
304 regression model, describing the probability of rockfall in the Central European low mountain ranges as a function of
305 meteorological (pre-) conditions, was fitted using ~~to~~ the Rupp and Damm (2020) database of rockfall events. To find the
306 optimal statistical model, a large number of models including different atmospheric predictors and interaction terms between
307 the predictors were compared. The best model was selected based on the logarithmic skill score determined during cross
308 validation. The best-performing model includes across-site percentile of a fissure water proxy D (precipitation minus potential
309 evaporation determined for the last 5 days), the local percentile of daily precipitation and the binary information if a freeze-
310 thaw cycle has occurred within the last 9 days. It also considers the interaction between daily precipitation and D. ~~incorporates~~
311 ~~the compound nature of such events~~ By including several meteorological parameters the statistical model describes the
312 ~~multivariate compounding- nature (multivariate compounding) of rockfall initialization. By and taking preconditions into~~
313 ~~account the preconditionedtemporally compounding component is addressed.~~ ~~into account preconditions (temporal~~
314 ~~compounding). The predictors for the statistical model are the across-site percentile of a fissure water proxy D (precipitation~~
315 ~~minus potential evaporation determined for the last 5 days), the local percentile of daily precipitation and the binary information~~
316 ~~if a freeze-thaw cycle has occurred within the last 9 days. Using the statistical model, a probability for a rockfall event can be~~
317 ~~determined for each day from the meteorological conditions of the previous 9 days and the day itself. Details of the statistical~~
318 model can be found in Nissen et al. (2022).

319 2.10 Convective cluster events of the summer 2018

320 Convective cluster events (CCEs) are spatially connected areas of intense lightning activity that occur simultaneously in the
321 same geographic region. CCEs can be detected using the Spatial-Temporal Density-Based Spatial Clustering of Applications
322 with Noise (ST-DBSCAN) algorithm (Ester et al., 1996; Birant and Kut, 2007). The data used are cloud-to-ground lightning
323 strokes from the European Cooperation for Lightning Detection (EUCLID) network (Schultz et al., 2016). ST-DBSCAN is
324 further developed and specifically adapted for the detection of spatio-temporal clustering of lightning strokes (Augenstein et
325 al., 2023). The algorithm identifies arbitrarily shaped clusters in a set of given points, which in this case are spatio-temporally
326 close lightning strokes. For the identification of CCEs, thresholds from sensitivity studies have been used, i.e., if at least 40
327 lightning strokes occur within 20 minutes and 50 km, single lightning ~~strikes~~ ~~strokes~~ are marked belonging to a CCE. These
328 thresholds have proven to be an “optimal” balance to distinguish between lightning clusters and noise.

329 2.11 Occurrence Frequency of extreme compound events from recent to near-term future climate conditions

330 The estimation of the projected changes in the frequency of CEs from recent to near-term future climate conditions is based
331 on the 30-member CMIP6 MPI-GE (Olonscheck et al., 2023). The historical and SSP5-8.5 (Riahi et al., 2017) simulations for

332 the periods 1975-2025 and 2025-2075 are used, representing climate conditions that for the CMIP6 MPI-GE range from about
333 1 to 3 °C increase in global mean surface temperature since pre-industrial times (Olonscheck et al., 2023). The projections
334 cover Germany and more specifically the region defined by the 4°-16° E and 45°-55° N latitude-longitude domain. The
335 compound heat and drought ~~events (years~~ are defined by the cumulative precipitation from May to October and the mean daily
336 maximum temperature ~~in summer (from~~ June to August), spatially averaged over Germany. Extreme compound hot and dry
337 years exceed the 20-year return levels for both precipitation deficit and maximum temperature individually, defined as the 5th
338 and 95th percentiles, respectively, for the period 1975-2025. The compound precipitation-wind ~~years events~~ are defined on the
339 winter (December to February) daily mean precipitation and daily maximum surface wind. The selection of events is based on
340 the exceedance of the 98th percentile for wind and precipitation during the period from 1975 to 2025. For each grid cell, wind
341 and precipitation events are identified when they exceed this threshold on the same day, while for precipitation alone, the
342 exceedance can occur either on the same day or the day after.~~The selection of events is based on the exceedance of the 98th~~
343 ~~percentile for the period 1975-2025 and each grid cell on the same day for both variables or the day after for precipitation only.~~
344 The cumulative effect for the whole season is the sum of all daily occurrences over all winter days and each grid cell. Extreme
345 compound wind and precipitation years exceed the 20-year return levels for precipitation and wind individually, defined as the
346 95th percentiles of each variable for the period 1975-2025.

347 **2.12 Representation of moisture availability of 2018 in model simulations**

348 The performance of model simulations in realistically representing drought conditions like those of 2018 and the 2018-2020
349 three-year drought cluster of events is assessed based on the estimated trend of the warm season (March to August) moisture
350 availability in Germany. Drought conditions are described with the SPEI index (Vicente-Serrano et al., 2010) for observations,
351 using ERA5 data (Hersbach et al., 2020) for the period 1979-2019, and for bilinearly interpolated (regular 0.5° lon-lat grid)
352 and extended to 2021 ensemble simulations of CMIP5 (Taylor et al., 2012; Aalbers et al., 2023) global circulation models and
353 of EURO-CORDEX 0.11° (Giorgi et al., 2009) regional ~~multi-model~~ multi-model ensemble for the historical (1950-2005) and
354 the near-to-mid-term future (2006-2070) periods under RCP8.5. The linear trend of the 3-year running mean for the March to
355 August intervals is calculated over the periods 1975-2021 for the simulations (~~or~~ 1979-2019 for ERA5) and 2022-2070 in order
356 to account for the transition from dimming to brightening regime in the 1970s (Wild, 2009, 2016).

357 **3 Compound events in the year 2018**

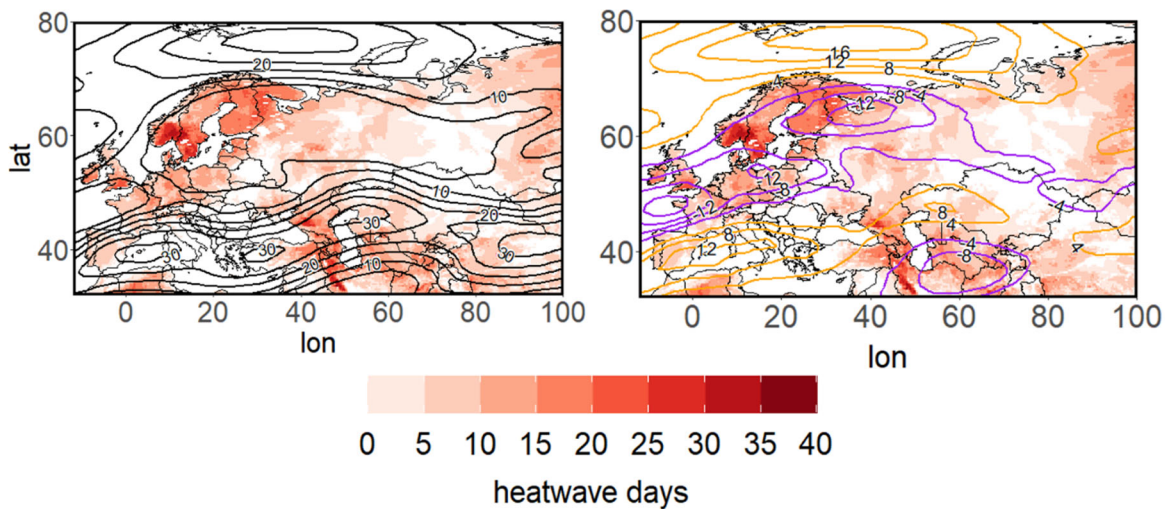
358 **3.1 Temperature-precipitation compound events during 2018**

359 The exceptionally hot and dry conditions in 2018 extended over larger areas including central and northern Europe and were
360 associated with impacts on various economic sectors (e.g. Toreti et al., 2019a; Zscheischler and Fischer, 2020; Bastos et al.,
361 2023; Conradt et al., 2023; Shyrokaya et al., 2024). ~~We study this exceptional year and the series of extremes and CEs in a~~

362 sequence of the large scale, their detection and spatial representation as well as the long term impacts on soil moisture both at
363 the continental scale and the consequent agriculture and forestry impacts at the national scale.

364 3.1.1 Drivers of the hot summer of 2018

365 The 2018 heatwave was a spatially CE featuring concurrent heatwaves in Scandinavia and central Europe (Spensberger et al.,
366 2020; Rousi et al., 2023). ~~Studies have explored the potential attribution of the strong heatwave of 2018.~~ Prior to the 2018
367 heatwave, a ~~striped~~~~stripped~~ high-pressure system formed over northern Europe in late June, during a combination of the
368 positive phase of the North Atlantic Oscillation and the Rossby Wave 7 pattern (Drouard et al., 2019; Kornhuber et al., 2019).
369 Figure 1 presents the jet stream state during the 2018 summer and the heatwave day frequency for each grid point over the
370 Eurasian sector. During the intense European summer heatwave, a large blocking system at 500 hPa, and a double jet stream
371 configuration is visible in the 250 ~~mb~~-hPa zonal wind field (Kornhuber et al., 2019; 2020; Rousi et al., 2023, see Methods
372 section 2.1). Heatwave hot spots over Europe coincide with areas of weak winds between the polar and subtropical jets. Such
373 large-scale atmospheric conditions are conducive to the occurrence of extreme events over Europe, in particular to heatwaves
374 near the centre of the blocking system (see Kautz et al., 2022 for a review). In particular, the hot summer of ~~summer~~-2003
375 (western/central Europe, Luterbacher et al., 2004; Fink et al., 2004; Fischer et al., 2007; García-Herrera et al., 2010) and 2010
376 (heatwave over western Russia, Barriopedro et al., 2011; Di Capua et al., 2021; Rousi et al., 2022) were characterised by
377 similar large-scale conditions.

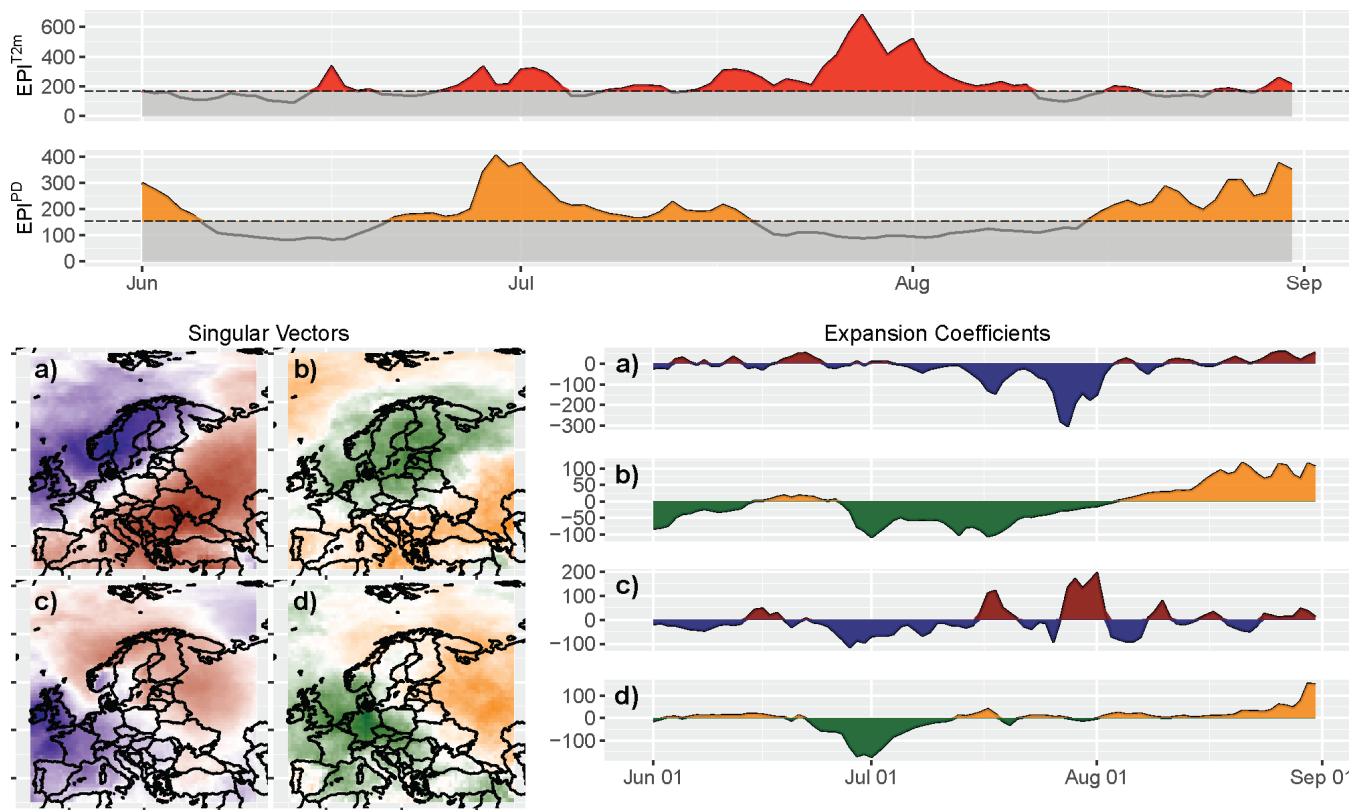


378
379 **Figure 1: Jet stream state (contour lines) and heatwave days in summer 2018 (shading). Left: zonal wind at 250 hPa (black contours**
380 **from 5 m/s to 30 m/s every 5 m/s); Right: zonal wind anomalies at 250 hPa (anomalies based on 1979-2020 July climatology and**
381 **plotted with contours from -16 m/s to 16 m/s every 4 m/s, negative anomalies are shown in purple contours and positive in orange)**
382 **for the period 4-25 July 2018, the longest period of consecutive double jet states. All fields stem from ERA5 reanalysis data (Hersbach**
383 **et al., 2020).**

384 **3.1.2 Detection of spatial patterns of extreme events**

385 During the summer 2018, large-scale temperature (T2m) and precipitation deficit (PD) patterns characterize the exceptional
 386 conditions. Figure 2 shows the analysis of ~~these patterns and~~ typical pattern of common extremes and their expression during
 387 the 2018 heatwaves at the European scale based on cross-TPDM and EPI (see Methods section 2.2).

388 In July-August 2018 the pronounced heatwave is accompanied by extreme EPI^{PD} preceding the heatwave for several days.
 389 This heatwave is considered the most prominent event in the period under consideration (see also Liu et al., 2020). The negative
 390 eigenvector anomalies of the second mode (Fig. 2a,b bottom left) mostly cover the regions identified as heatwave spots in
 391 Figure 1. Thus, ~~the negative~~ anomalies in the second mode expansion coefficients (Fig. 2a,b bottom right) indicate the
 392 beginning of the heatwave, which initially affected northern Europe (i.e., Finland, Norway, and northwestern Russia). From
 393 mid of June onwards, there were extremes in PD, particularly in Central Europe, as indicated by the third mode of the expansion
 394 coefficient (Fig. 2c,d bottom right). By the end of July 2018, the heatwave extended to Central Europe as evidenced from the
 395 abrupt change of sign in the third mode expansion coefficient (Fig. 2c,d bottom right).



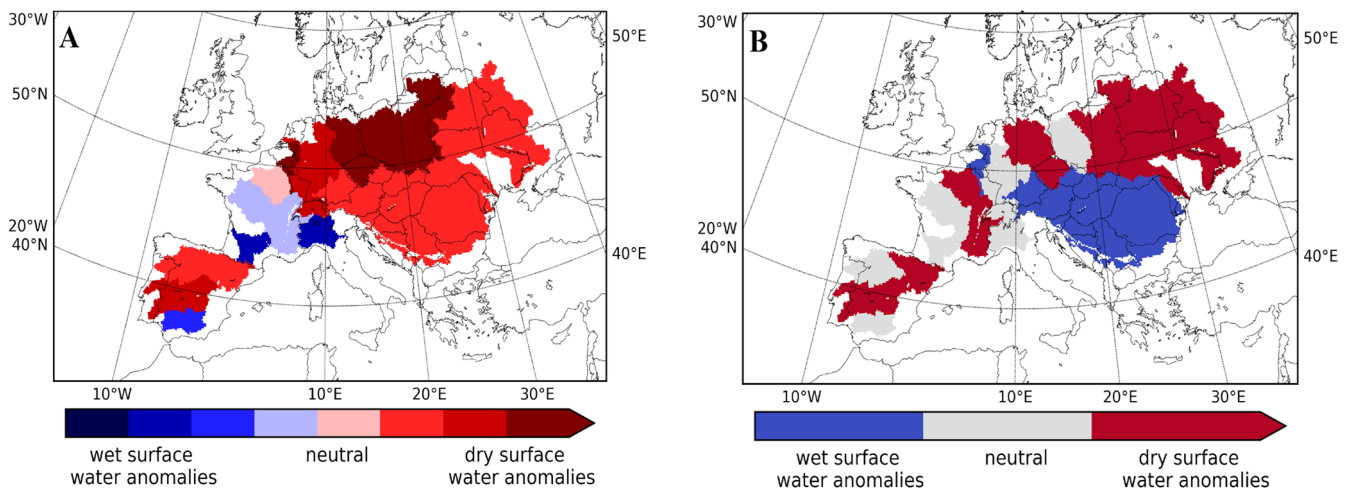
396
 397 **Figure 2: Top: Extreme Pattern Index (EPI) for T2m surface temperature (EPI^{T2m} , red) and precipitation deficit (EPI^{PD} , orange)**
 398 **for northern Hemisphere 2018 summer months. Values exceeding the 80th percentile are considered to identify extreme events in**
 399 **PD and T2m from EPI and are highlighted in red/orange, respectively; Bottom left: second (a, b) and third (c, d) singular vectors**
 400 **(CVs) associated with large-scale temperature (blue/red) and precipitation deficit (green/orange) pattern; Bottom right: second (a,**

401 **b) and third (c, d) expansion coefficient for northern hemisphere 2018 summer months. Positive values are plotted in red/orange**
402 **and negative values in blue/green.**

403 **3.1.3 Surface water storage of the dry summer of 2018**

404 The high temperature in 2018 was mainly due to increases in the amount of net surface radiation caused by the clear skies
405 associated with reduced precipitation (Liu et al., 2020). Germany experienced a strong increase of net radiation of
406 approximately +31%. Liu et al. (2020) report that land cover played a critical role in determining the occurrence and strength
407 of soil moisture-temperature coupling, i.e. cropland/grassland depletes soil moisture more readily than forests, thereby
408 triggering a more rapid release of sensible fluxes a major feature observed during the 2018 heatwave. During the 2018
409 heatwave, because of different soil moisture conditions, latent flux in Germany decreased by 12% and sensible flux
410 significantly increased by 122% (Liu et al. 2020). Further, Bastos et al. (2020) used 11 vegetation models and showed that
411 spring conditions promoted increased vegetation growth, which, in turn, contributed to fast soil moisture depletion, amplifying
412 the summer drought. Figure 3 presents the groundwater memory in the summer 2019 of the ensuing hydrological year
413 2018/2019 for each of the 20 European river basins on the following year's summer surface water storage (S_u).

414 The ensemble simulations indicate that following the 2018 drought the conditional probability that the autumn of the
415 hydrological year 2018/2019 (August to November 2018) is anomalously dry $p(S_{u,d})$ is 95.5% with a $100 \pm 0.0\%$ confidence
416 with respect to the climatological variability. In the following seasons, $p(S_{u,d})$ and the associated confidence decrease due to
417 the increasing influence of the uncertainty in the atmospheric conditions. Specifically, for winter $p(S_{u,d})$ is 81.8% with a
418 confidence of $99.5 \pm 0.3\%$, for spring (March to May 2019) 63.6% with a confidence of $80.2 \pm 6.0\%$ and for summer (June to
419 August 2019) of the hydrological year 2019/2020 $p(S_{u,d})$ is 68.2% with a confidence of $90.1 \pm 3.7\%$ with respect to the
420 climatological variability. Without considering the groundwater storage memory effect, a probability of a dry surface water
421 anomaly $p(S_{u,d})$ of $\sim 50\%$ would be expected due to the atmospheric uncertainty accounted for in the ensemble of realisations
422 at the interannual time scale. Taking drought as a precondition for S_u on this scale, the analysis shows that even one year later
423 a $p(S_{u,d})$ of 68% is still well above 50% at a confidence level of $90 \pm 4\%$. Thus, statistically, groundwater storage takes longer
424 than a year to fully recover from a drought influencing surface water storage, independent of the ambient atmospheric
425 conditions (Lorenz et al., 2010; Orth and Seneviratne, 2012; Song et al., 2019). Recent evidence points to the ~~fact that~~~~fact, that~~
426 the impact of global warming on soil moisture drought severity in west-central Europe such as the case in 2018 is increased.
427 The drought risk is strongly enhanced by the drought intensification and increase in frequency, yielding shorter recovery time
428 between events for nature and society (Aalbers et al., 2023).



429

430

431

432

Figure 3: Averaged impact of the yearlong 2018 drought on the following year's summer (June to August 2019) surface water storage (S_u) anomaly per river basin (see Methods section 2.3). A: S_u anomaly in 2018 for each river basin in quartiles; B: S_u anomaly in the summer (June to August 2019) after 2018 initial conditions and (ensemble) mean of 22 atmospheric conditions.

433

3.1.4 Soil moisture of the dry summer of 2018

434

435

436

437

438

439

440

441

442

443

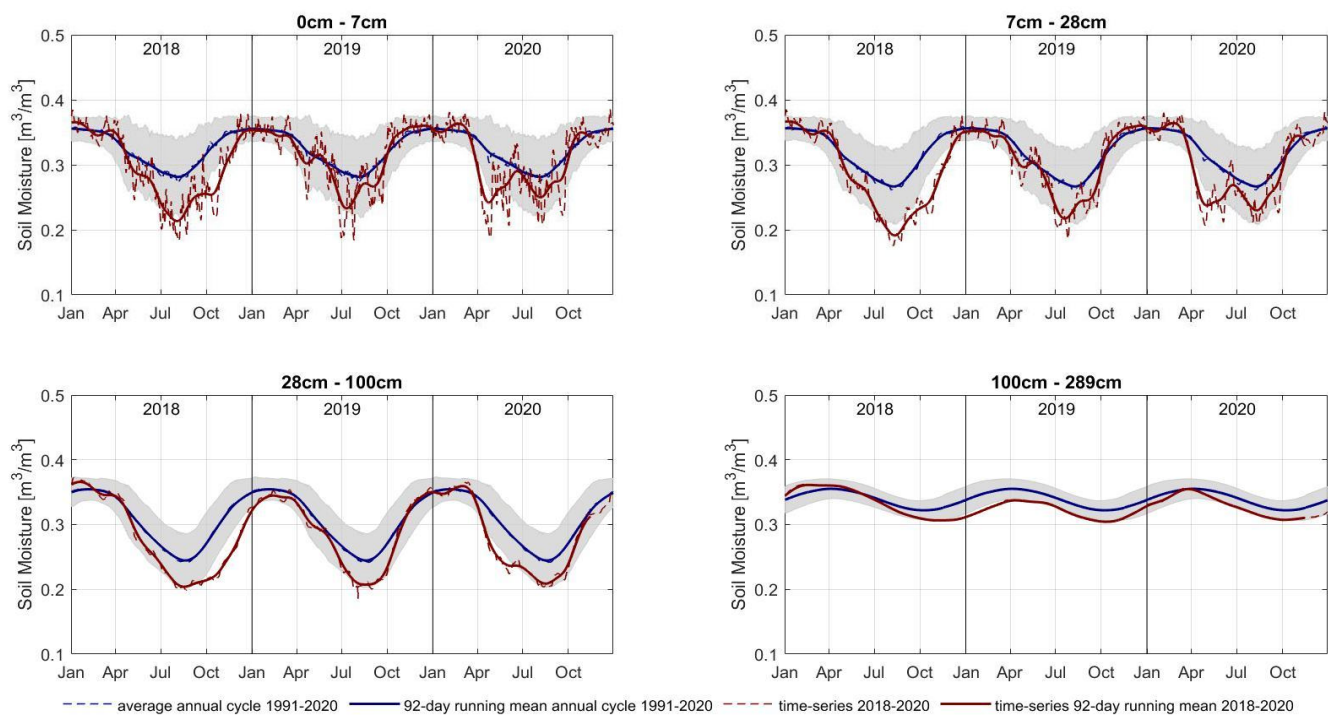
444

445

446

447

To address sectoral impacts (e.g. Conradt et al., 2023), we focus on the effects of the 2018 drought on agriculture and forestry in Germany. For this purpose, the temporal evolution of soil moisture deficits at different depths from the ERA5 dataset and agricultural data from German national institutes such as the Statistisches Bundesamt (Destatis) are analysed. Focusing on the temporal evolution of soil moisture, a deficit developed during the spring and early summer of 2018 (Rousi et al., 2023), which also reached the lowest soil layer with a temporal delay of about three months, as shown in Fig. 4. The dryness in 2018 was more intense than the usual soil moisture variability in the period 1991-2020, as shown by the soil moisture dropping below the range of ± 1 standard deviation of the 1991-2020 mean soil moisture (shaded area). While the moisture in the three upper soil layers mostly recovered during the following winter 2018/2019, the moisture did not percolate down to the lowest soil layer, which remained in a dry anomaly. The recurrent drying of the upper layers in spring and summer 2019 inhibited considerable infiltration, so that the moisture deficit of the lower soil layer persisted until winter 2019/20, when the relatively wet climatic conditions allowed a recharge of the lower soil layer moisture reservoir (Brakkee et al., 2022) and thus probably also of the groundwater (e.g., Brauns et al., 2020). Hence, the lack of soil moisture reached the entire soil column and thus the entire root zone of the vegetation during the summers of 2018 and 2019, placing the vegetation under soil moisture stress (Tijdeman and Menzel, 2021).



448

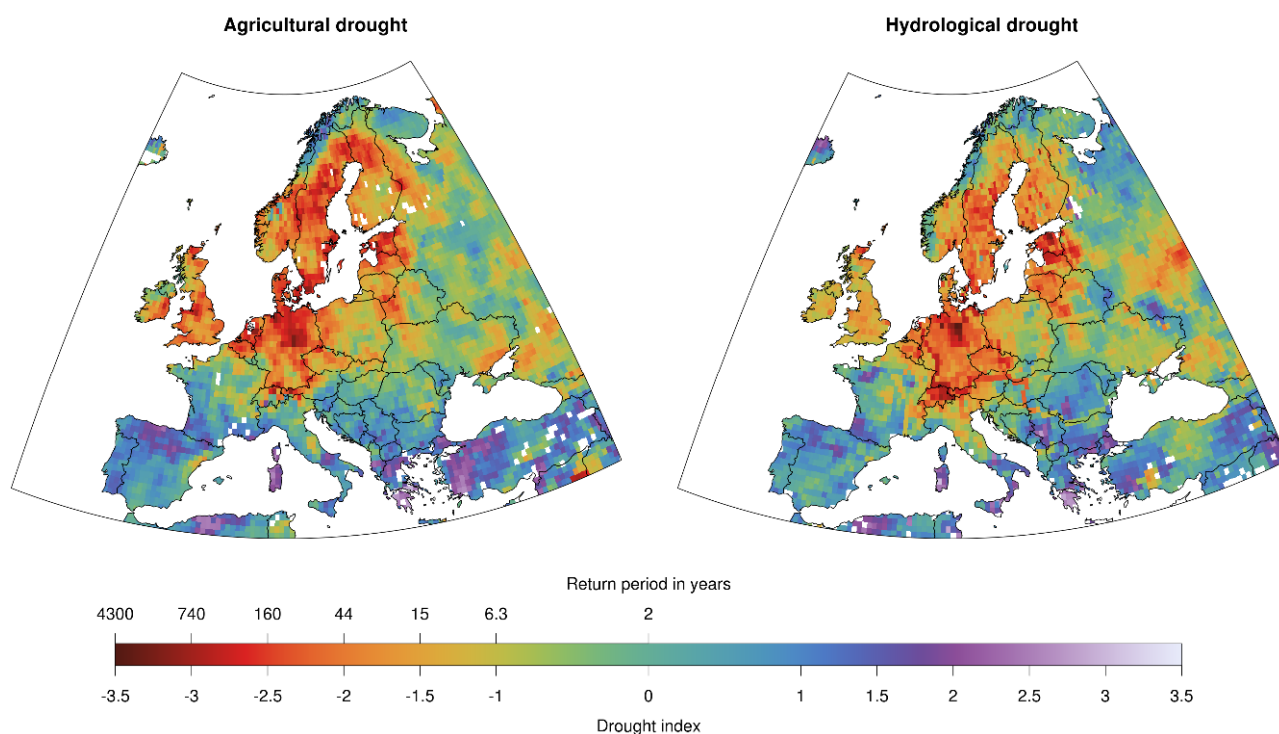
449 **Figure 4:** ERA5 soil moisture in four different layers from surface (0 - 7 cm) to a depth of 2.89 m (100 - 289 cm) with two intermediate
 450 layers 7 - 28 cm and 28 - 100 cm depth. The red dashed line denotes the daily mean and the solid red line denotes the 92-day running
 451 mean in 2018-2020. The annual cycle of soil moisture with a daily resolution (dashed blue line) and the average running mean (solid
 452 blue line) are also shown. The grey shading indicates a range of ± 1 standard deviation of soil moisture over the period 1991-2020
 453 indicating the normal year-to-year variability of the soil moisture.

454

455 3.1.5 Agricultural and hydrological drought of the year 2018

456 The anomalous abnormal soil moisture conditions are reflected in an anomalous abnormally low ET/PET ratio over the summer
 457 months (June, July, August), indicating a severe agricultural drought (Fig. 5, left). In almost the entire northern part of
 458 Germany, the agricultural drought index exceeds -2.5, which is equivalent to a return period of more than 160 years, an estimate
 459 associated with uncertainties. However, the agricultural drought is not limited to northern Germany but comprises large parts
 460 of central, northern, and northeastern Europe. The low soil moisture conditions also lead to a hydrological drought (low river
 461 flow) over the summer months (Fig. 5, right). However, the severity and spatial pattern of hydrological drought differs from
 462 the pattern of agricultural drought because propagation from soil moisture drought to hydrological drought takes time and
 463 typically leads to a lagged occurrence (Van Loon and Van Lanen, 2012) and a longer persistence (see section 3.1.3 on Surface
 464 water storage). Another reason is that hydrological drought can spread along the river network affecting regions unaffected by
 465 low soil moisture (e.g., along the Danube river in eastern Europe). Nevertheless, in many parts of Germany and northern
 466 Europe, agricultural and hydrological drought coincided in the summer of 2018 (Blauhut et al., 2022), affecting the possibility

467 to irrigate as a means to alleviate the agricultural drought. This provides an example of how co-occurring impacts (droughts)
468 can amplify each other to cause even greater secondary impacts (agricultural yields, see section 3.1.6 on Impact on the
469 agricultural production) in a similar way as co-occurring meteorological conditions trigger CEs.

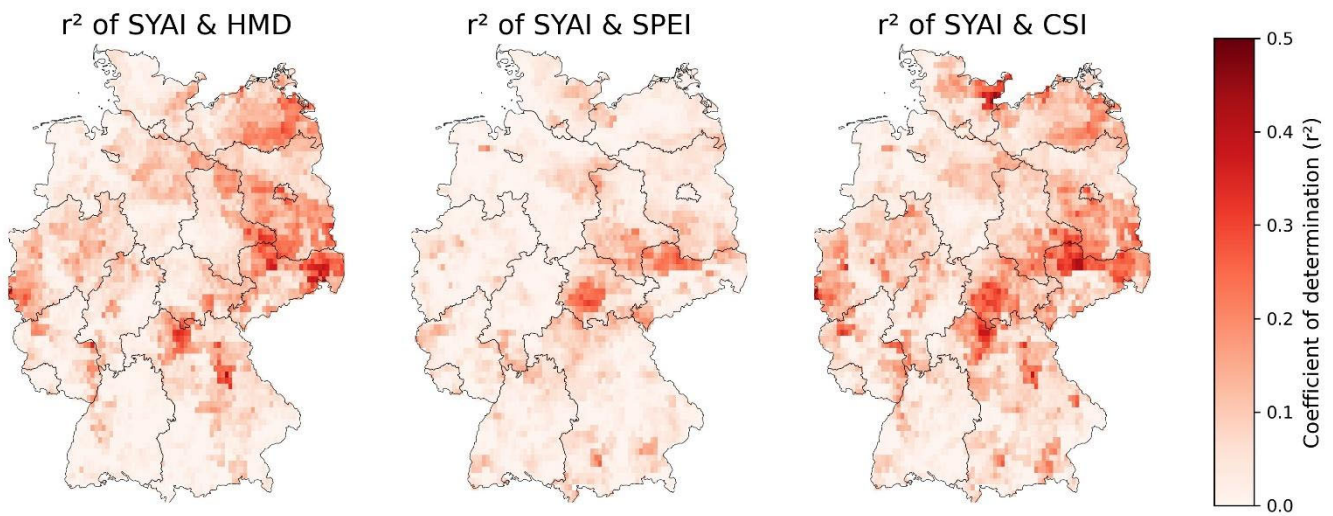


470
471 **Figure 5: Drought severity and return period of agricultural and hydrological drought during summer 2018. Note that drought**
472 **severity (as expressed by the drought index) and return period are closely related (see Methods section 2.5).**

473
474 **3.1.6 Impact on the agricultural production of 2018**

475 In Germany, the hot and dry spring and summer of 2018 had an unprecedented impact on crop yields. Extremely low crop
476 yields (Toreti et al., 2019a; Bellouin et al., 2020; [Conradt et al., 2023 for northeastern Germany](#)) led to large insurance claims
477 over agricultural losses and financial support requests by farmers from governments in Germany (EUR 340 million), Sweden
478 (EUR 116 million) and Poland (EUR 116 million) (D'Agostino, 2018; Munich Re 2019). [Winter wheat Yields-yields for winter](#)
479 [wheat](#) were more than 10% below the 30-year average and 13% below the previous three years. In some counties, yields were
480 more than 40% lower than in previous years. Regionally, winter wheat was particularly hard hit in eastern and northeastern
481 Germany, with an average loss of 22% compared to the last three decades. The HMD index and the SPEI indicate a severe
482 heatwave and drought respectively, which was most pronounced in central and northeastern Germany. Figure 6 shows the
483 explained variance of yield anomalies and the stress indices HMD, SPEI and CSI (see Methods section 2.6) revealing a strong

484 connection between these components. However, not all regions experienced such severe yield losses; winter wheat yield in
485 southwest Germany was hardly affected, with losses of only 1.2% compared to the last three-decade average. A hydrological
486 see-saw with rather wet conditions in southern Europe and the resulting yield increases characterise the unique combination
487 of climatic anomalies in Europe in 2018 (Toreti et al., 2019a). Winter wheat productivity was even positively affected in some
488 regions.



489
490 **Figure 6: Coefficient of determination of Standardized Yield Anomaly Index (SYAI) and stress indices Heat Magnitude Day (HMD),**
491 **Standardized Precipitation Evapotranspiration Index (SPEI) and Combined Stress Index (CSI) demonstrate the impact of heat,**
492 **drought and compound stress over the last three decades on winter wheat in Germany.**

493

494 3.1.7 Impact on the forests in 2018

495 The drought of 2018 was likely the largest source for severe forest disturbance in Europe for more than 170 years (Senf and
496 Seidl, 2021), especially in central and northern Europe (Buras et al., 2020). Consequently, in the summer of 2018, about 11%
497 of the central European forest area experienced early wilting (Brun et al., 2020), resulting in a large reduction in greenness
498 (Schuldt et al., 2020; the three aforementioned studies are based on NDVI data). The 2018 drought continued into 2019, making
499 the consecutive European droughts of 2018 and 2019 unprecedented in the last 250 years (Hari et al., 2020). The low soil
500 moisture content in 2018 and an increased water-vapour pressure deficit in the following two years were the main drivers for
501 the forest disturbances of about 4.74×106 ha in Central Europe (Senf and Seidl, 2021). The likely cause for these forest
502 damages was that trees under drought and heat stress experience carbon starvation (Bastos et al., 2020) and have risk for
503 embolism, which causes failures in water transport (Allen et al., 2015; Schuldt et al., 2016). The drought and heatwave in that
504 period facilitated outbreaks of bark beetle, enhancing the damage levels to forests. As such, insect outbreaks in Central Europe
505 had a 2-3-fold increase in annual losses between 2017 and 2018 (Hlásny et al., 2019) and extraordinary mortality and damage

506 occurred during 2018 in Sweden due to rapid beetle population growth (Öhrn et al., 2021). Although wildfires have decreased
507 on a global scale recently, Central Europe is likely to face larger and more frequent forest fires (Feurdean et al. 2020, Milanovic
508 et al. 2020; Carnicer et al., 2022), which can have severe environmental, economic and social consequences (Lidskog et al.
509 2019).

510 **3.2 Precipitation-wind compound events during 2018**

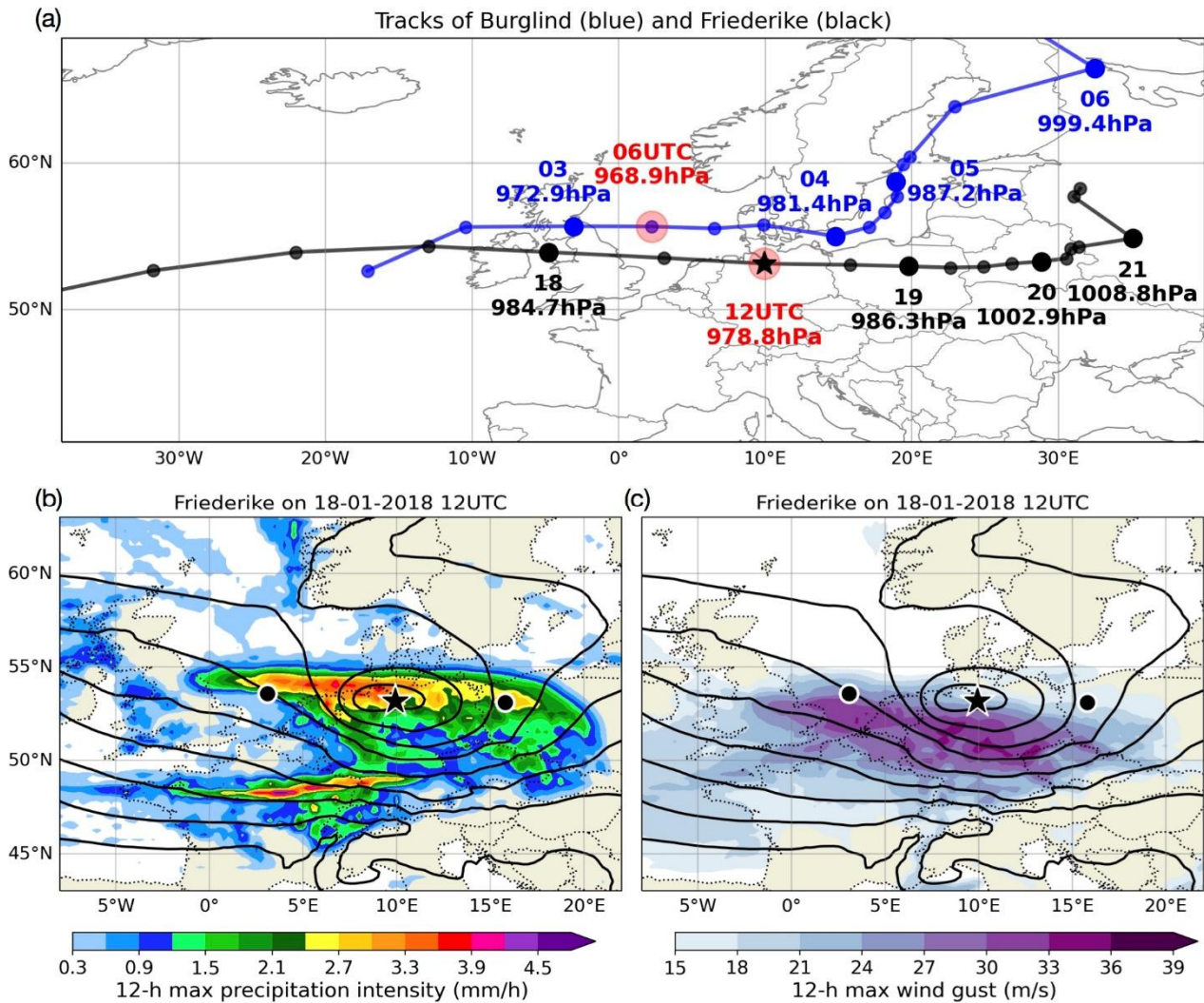
511 In this section, CEs that involve heavy precipitation and strong winds are described. Examples include two January windstorms
512 (Friederike and Burglind) and several weeks of convective activity in May and June of 2018.

513 **3.2.1 Loss and damage of compound vs. non-compound wind extreme events of the winter 2018**

514 On January 16, windstorm Friederike formed as a low-pressure system near Newfoundland. Within the next two days,
515 Friederike intensified and quickly travelled across the Atlantic (Fig. 7), losing its closed structure at 1800 UTC on 17 January.
516 Friederike re-intensified over the British Isles on 18 January while crossing the jet streak towards the northern jet exit region,
517 a behaviour favourable for intense windstorm development (e.g., Pinto et al., 2009). The storm moved eastward over the North
518 Sea, Germany and Poland, and weakened after 19 January over eastern Europe (Fig. 7a). Analysing the compound character
519 of Friederike around peak intensity using the hourly ERA5 reanalysis data (Fig. 7b,c), the typical near-surface wind and
520 precipitation structure of intense extratropical cyclones is found (e.g., Dacre et al., 2012). Strong 10 m wind gusts (maximum
521 values of 34 m/s relative to the Earth's surface) were present behind and to the right of the eastward moving cyclone centre.
522 Heavy precipitation occurred at both the warm front to the northeast of the centre, wrapping around as the cyclone approached
523 its mature stage, and along the east-southwest stretching cold front (Fig. S1a). During the 12 h period when Friederike passed
524 through Germany from 0600 UTC to 1800 UTC on 18 January, the persistently active warm front left a widespread footprint
525 near the northern edge of the cyclone centre (Fig. 7b) with ERA5 accumulated precipitation exceeding 17 mm. Meanwhile,
526 the cold front contributed to a high precipitation rate (> 4 mm/h based on ERA5) along a narrow west-east oriented band across
527 northern France and southern Germany (Fig. 7c). The co-occurrence of strong winds and heavy snowfall gave to this storm
528 the risk and damage characteristics of a CE (Fig. 7b,c). The highest damages were reported in Ireland, Great Britain, northern
529 France, Belgium, the Netherlands, Germany, Czech Republic and Poland, where gust measurements suggested wind speeds of
530 the order of 100 – 150 km/h. At higher altitudes the observed wind gusts reached 173 km/h at the Sněžka in Czech Republic
531 and 203 km/h at Brocken in Germany (Haeseler et al., 2018). Wind and snowfall associated with Friederike caused further
532 traffic disruption, power outages, property damage including falling trees, and several deaths. Friederike was the strongest
533 storm affecting central Germany since windstorm Kyrill in 2007.

534 Another CE affecting Germany in the same month was the windstorm Burglind, which formed on the 2nd January 2018. The
535 depression intensified rapidly as it moved eastwards towards the British Isles (Fig. 7a). It reached a peak intensity of 968.9
536 hPa at 0600 UTC on 3 January 2018 over the North Sea, followed by a weakening over the Baltic Sea. The long active cold
537 front affected a large area of western Europe (Fig. S1b). Heavy precipitation with daily values > 30 mm led to rapid snowmelt

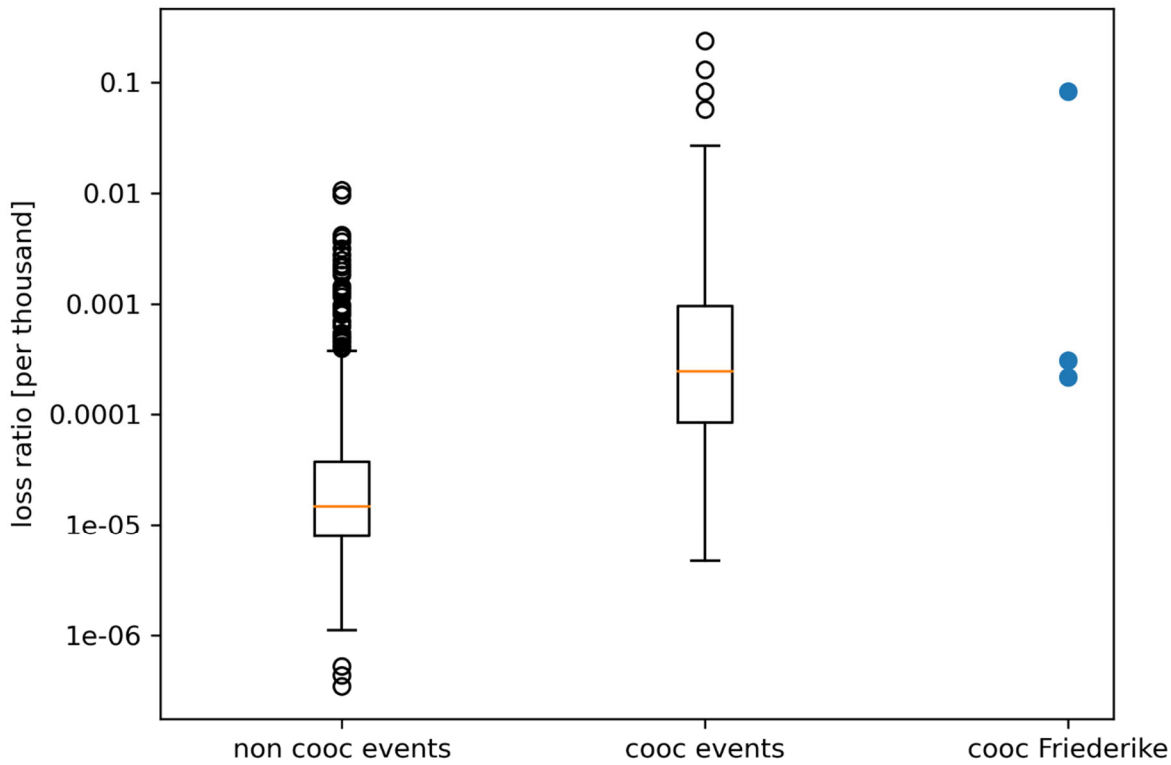
538 and massive flooding in many regions. Around the time of the peak cyclone intensity, widespread areas were simultaneously
 539 affected by high precipitation intensities (> 4 mm/h) and high wind gust (~100km/h) (Fig. S1c,d). Further detailed information
 540 on Burglind can be found in Eisenstein et al. (2022, see their section 5). Compared to storm Friederike, the compound features
 541 of Burglind were more strongly shaped by orography.



542
 543 **Figure 7: (a) Cyclone tracks of windstorms Friederike (black) and Burglind (blue) in January 2018. Big circles show locations at**
 544 **0000 UTC on the day as indicated, with the central pressure noted below. Red circles indicate their lifetime peak intensity based on**
 545 **the minimum pressure. (b) Mean sea level pressure (thick contours; increasing from 960 hPa with 5 hPa intervals) at 1200 UTC on**
 546 **18 January 2018 (location of Friederike shown by the star) and maximum precipitation intensity (shaded) during the period 6 h**
 547 **before and after (locations shown by black circles). (c) Same as b, but for the wind gust at 10 m height (shaded). All fields are derived**
 548 **from the ERA5 reanalysis (Hersbach et al., 2018).**

549

550 Although the co-occurrence of extreme wind and precipitation is discussed in previous studies for specific events (e.g. Fink et
 551 al., 2009 for storm Kyrill) or globally (Martius et al., 2016; Messmer and Simmonds, 2021), there are no studies so far
 552 quantitatively evaluating the effect in terms of loss damage. To distinguish between single extreme wind speed events and
 553 compound extreme wind speed and precipitation events, we follow the definition of Martius et al. (2016), where both variables
 554 are considered simultaneously (see the Methods section 2.7). The loss damage distribution for compound and non-compound
 555 events determined from loss data of the GDV is depicted in Fig. 8. For Friederike, there are three days where a co-occurrence
 556 of wind and precipitation extremes can be identified over Germany, i.e. 17, 18, and 19 January 2018. The loss ratio for these
 557 three days is marked with blue dots in the right column of Fig. 8. The GDV Naturgefahrenreport (2019) reports 900 Million €
 558 loss damage for Germany with respect to Friederike. To this date, it was the most damaging winter storm of the last ten years.

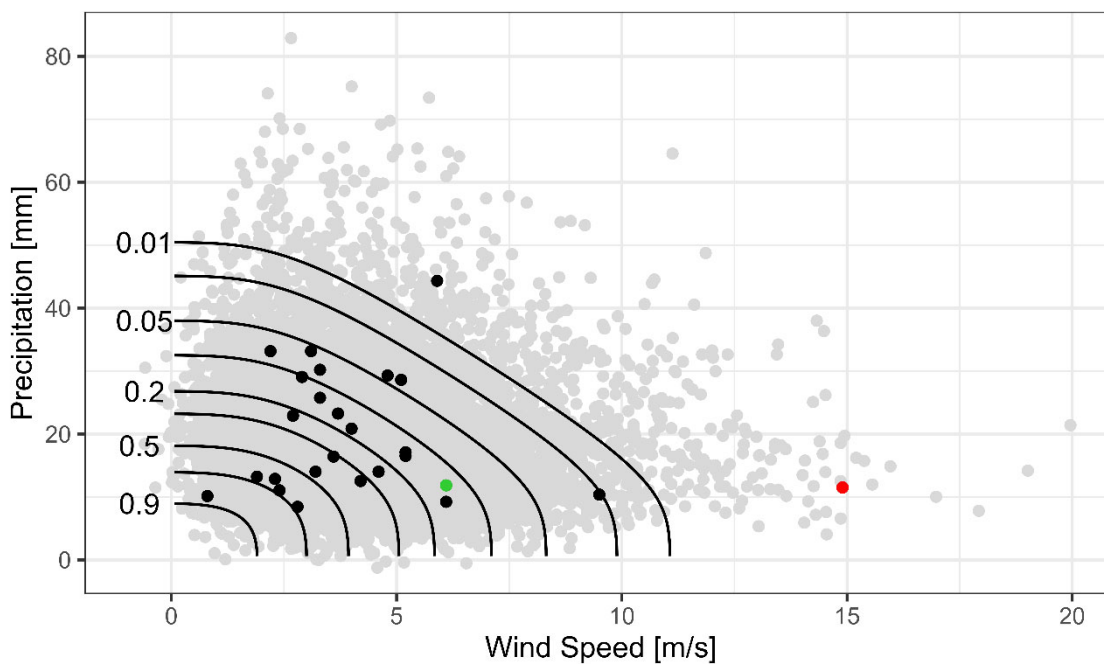


559
 560 **Figure 8: Loss ratio of residential buildings [per thousand] accumulated over Germany for winter events from 1997-2016. Each dot**
 561 **represents one day. Left (non cooc events) bar shows all days which cannot be linked to co-occurrence (cooc) of both extreme wind**
 562 **and precipitation, i.e. single extreme events. Middle bar (cooc events) shows all days which can be linked to co-occurrence of extreme**
 563 **wind and precipitation. Right bar shows the three days for the co-occurrence during windstorm Friederike. The loss ratio is defined**
 564 **by loss normalized with the local sum of insured values.**

565

566 **3.2.2 Concurrent heavy rain and storm extremes – estimation of probability of event occurrence**

567 In a detailed analysis of the probability of co-occurrence of extremes, based on copulas (see Methods section 2.8), the annual
568 maximum values of hourly precipitation and wind speed data at the station Münster/Osnabrück Airport of DWD that are
569 available since 1996 were analysed. The records show an increase in the intensity and frequency of the variables but lack a
570 statistically significant trend. The occurrence probabilities for concurrent precipitation and wind extreme events are shown by
571 the black isolines in Fig. 9. The grey dots are pseudo-observations (artificial precipitation and wind combinations generated
572 using the copula function), while the black, red and green dots mark the observed CEs at the station for each year and the green
573 dot represents Friederike. The distribution of the dots illustrates that - depending on the precipitation duration – wind or
574 precipitation, individually, may not be extreme. A counterexample is the year 2020 windstorm Sabine (red dot; internationally
575 known as Ciara) for which the simultaneous wind and hourly precipitation values both correspond to the respective annual
576 maximum event of that year. The location of the dots relative to the isolines define the return period of the event, where the
577 return period of windstorm Friederike at the station Münster/Osnabrück exceeded 5 years and the one of windstorm Sabine
578 100 years.

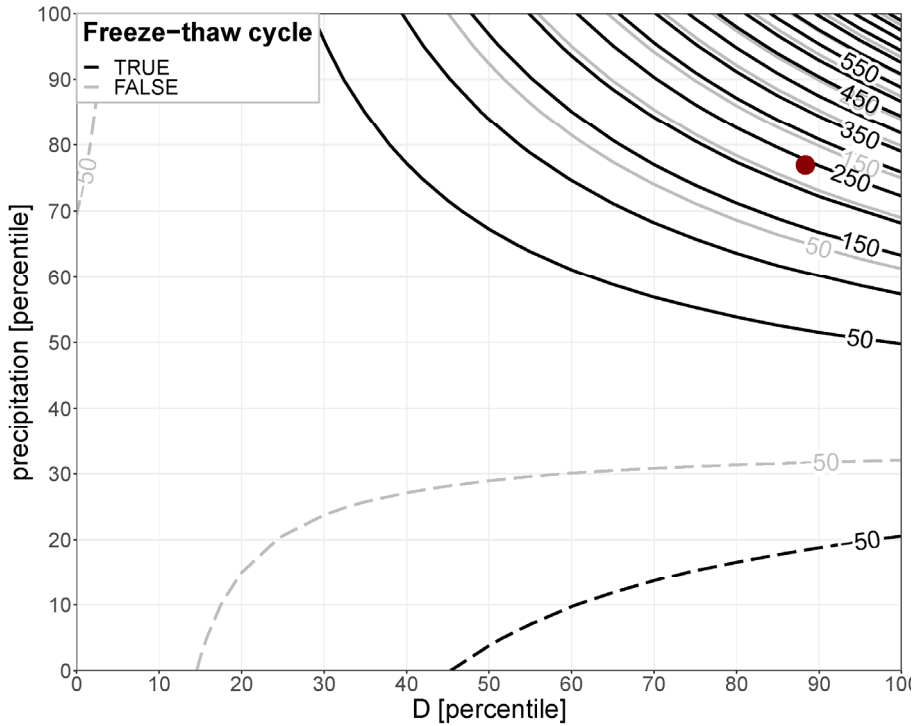


579
580 **Figure 9: Multivariate analyses for the temporal compound event heavy precipitation and strong wind determined with Copula**
581 **functions: quantile isolines (lines of equal probabilities), observed event combinations (black dots) and the pseudo-observations (grey**
582 **dots). Green dot represents storm Friederike (2018) and red dot storm Sabine (2020).**

583

584 3.2.3 Rockfall events

585 Another hazard with CE triggers observed in connection with Friederike was a rockfall event. Although wind is normally not
586 considered as one of the triggering factors (D'Amato et al., 2016), such events may also occur as the consequence of the
587 precipitation associated with the windstorm. It is well known that heavy precipitation can initiate landslides and rockfall events
588 (e.g. Nissen et. al., 2022). Slope susceptibility is influenced by pore water/fissure water preconditions, rendering them events
589 with multivariate and temporally compounding triggers. With respect to rockfall, another potentially triggering factor are
590 freeze-thaw cycles prior to the event. In terms of reported hill slope failures, storm Burglind was more effective than storm
591 Friederike. For storm Friederike, only one rockfall event is registered in the landslide database for Germany. The event
592 occurred near Göttingen in Lower Saxony. Figure 10 shows the relationship between the predictors (across-site percentile of
593 a fissure water proxy D -precipitation minus potential evaporation determined for the last 5 days-, the local percentile of daily
594 precipitation and the binary information if a freeze-thaw cycle occurred within the last 9 days) and the rockfall probability
595 expressed as percentage change with respect to the climatological probability. The red dot indicates the conditions on the 18th
596 January 2018 in the area of the event associated with Friederike. The soil at the location was still wet after storm Burglind at
597 the beginning of month and the fissure water (proxy D) at its 83rd percentile. The daily precipitation on the day of the event
598 was 4.5 mm (REGNIE data, Rauthe et al., 2013), which corresponds to the 77th percentile for the given location, assuming
599 immediate melting of the reported snow due to the above freezing air temperature at the event location. The probability of a
600 rockfall event was further increased by pre-event thawing conditions. The logistic regression model suggests that the
601 probability of rockfall on that day was increased by almost 250% (3.5 times more likely) compared to the long-term
602 climatology.



603

604

605

606

Figure 10: Rockfall probability expressed as percentage change with respect to the climatological probability (isolines) as a function of moisture preconditions (D), daily precipitation and preceding freeze-thaw cycles. The red dot marks the conditions in the vicinity of Göttingen (Lower Saxony) on 18th January 2018.

607

3.2.4 Convective cluster events of the summer 2018

608

609

610

611

612

613

614

615

616

617

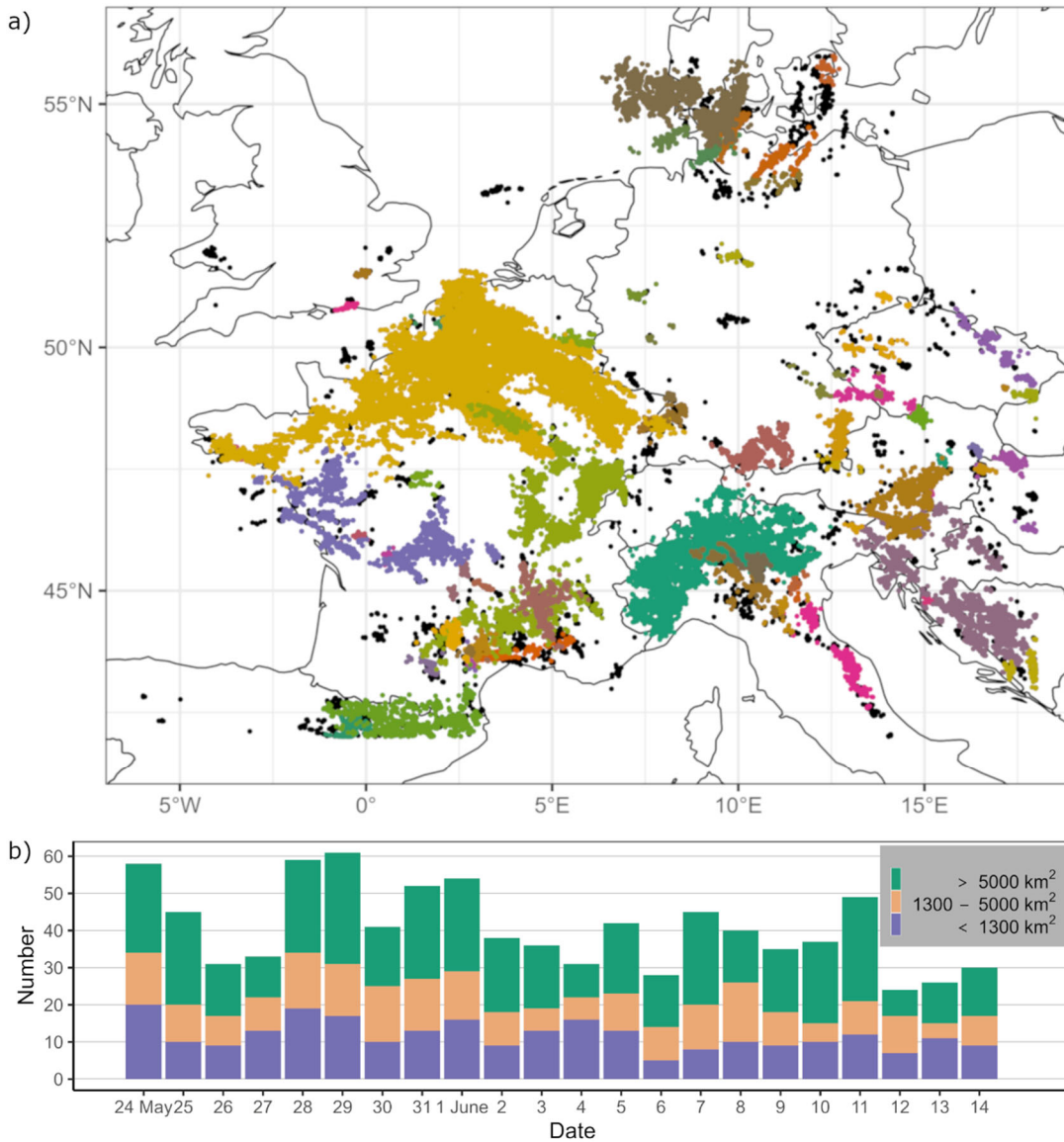
618

619

620

The spatially as well as temporally compounding nature of severe convective storms (SCSs) can be demonstrated on the example of a three-week series of SCSs in western and central Europe from 22 May to 12 June 2018 leading to the unusual high temporal accumulation of CCEs lasting several days (Fig. 11). During this period, an exceptional persistence of reduced stability combined with sufficient moist air masses caused high thunderstorm activity daily in France, Belgium, Netherlands, Luxembourg, Germany, Switzerland, and/or Austria, associated with precipitation accumulations of up to 80 mm/h within 1 hour and several flash floods (Mohr et al., 2020). The temporal compounding nature of the serial clustering of SCSs over several days to weeks over the same geographic region may increase the probability of flooding and damage. Figure 11b shows a large amount of identified CCEs, especially those with large spatial extent (> 5000 km²), during a three-week period over western and central Europe indicating high thunderstorm activity whose accumulation was unusual (Piper et al., 2016; Mohr et al., 2020). The repeating occurrence is caused by persistent synoptic conditions that favour thunderstorm development over several days to weeks. The presence of atmospheric blocking has been found to be highly conducive to such prolonged thunderstorm episodes, which typically occur on its western and /or eastern flanks (Piper et al., 2016; Mohr et al., 2020; Kautz et al., 2022). Based on statistical analyses, Mohr et al. (2019) found that a block over Scandinavia or over the Baltic Sea

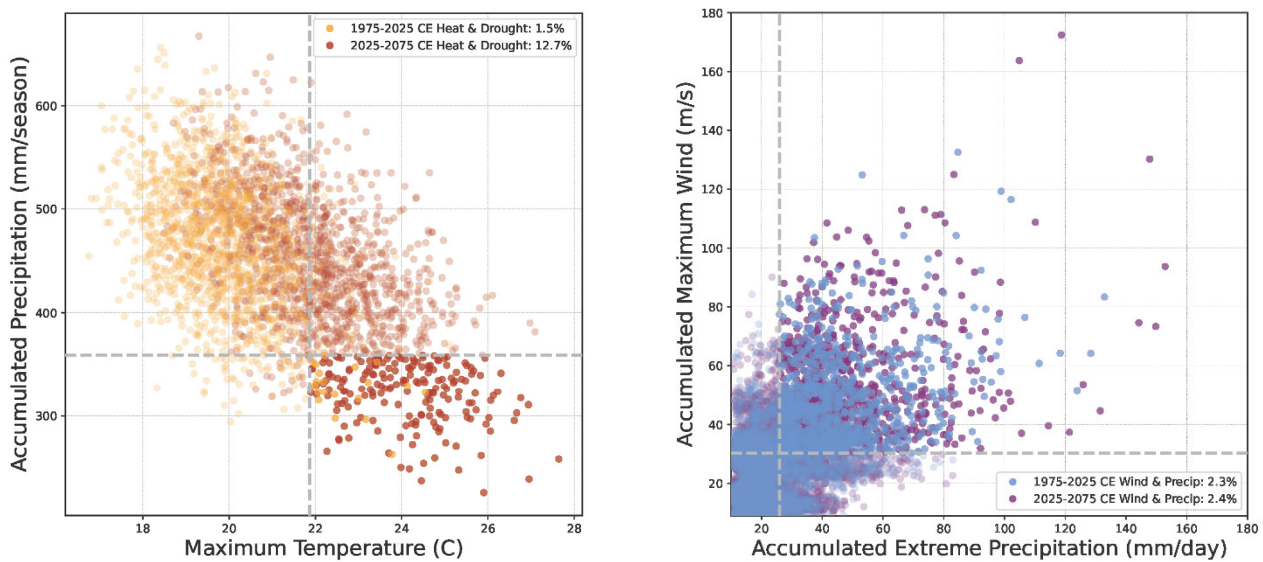
621 favoured the occurrence of thunderstorms in western and central Europe along the western flank of the blocking system due
 622 to of southwesterly advection of warm, moist, and unstable air masses. It is expected that low-frequency modes of climate
 623 variability like North Atlantic Oscillation (NAO) or East Atlantic Pattern (EA) could also have an impact on clustered
 624 thunderstorm activity over several days (Piper et al., 2019), as these patterns are connected with atmospheric blocking.



625
 626 **Figure 11: (a) Lightning strokes on the 28 May 2018 in western and central Germany. Each colour represents a convective cluster**
 627 **event (CCE) resulting from the ST-DBSCAN method (see Methods section); black dots represent lightning strokes identified as**
 628 **noise. (b) Daily number of CCEs between the thunderstorm episode from 22 May to 12 June 2018. The colours represent CCEs of**
 629 **different sizes. Note: clusters that overlap are separated in time.**

630 4 Compound events under climate change

631 In this paper, we have analysed in detail several extreme events that have affected Europe within the calendar year of 2018,
632 starting with the windstorm series in January, followed by a period of heavy thunderstorms in May/June and extended heatwave
633 in July and August which affected various parts of Europe, and the associated drought effects extended well into the autumn
634 season. Our analysis clearly revealed the multi-variate and complex characteristics of the events, and thus they can undoubtedly
635 be classified as CEs. ~~T~~Within ~~clim~~Xtreme, the analysis of compound variables was used as a tool to investigate the impacts of
636 man-made climate change. For the two overarching compound types collected in this contribution (hot and dry; wet and windy)
637 we now analyse possible changes of their frequency of occurrence under future climate conditions. Recent studies have
638 provided evidence that regionally extreme hot and dry conditions such as the summer 2018 are expected to become more
639 frequent in the future (e.g., Toreti et al. 2019a; Zscheischler and Fischer, 2020; Aalbers et al., 2023; van der Wiel et al., 2021;
640 Bevacqua et al., 2023). Figure 12 shows a comparison of the occurrence of CEs under recent (1975-2025) climate conditions,
641 with a global mean surface temperature of 1 °C above pre-industrial levels, and under future (2025-2075) conditions of 3 °C
642 above pre-industrial levels, based on the 30-member CMIP6 MPI-GE under SSP5_8_5 (see Methods section 2.11). For drought
643 and heat events, our analysis reveals a clear increase in both the frequency and intensity of extreme compound heat and drought
644 years (Fig. 12, left). Over the past 50 years, extreme compound heat-drought events have occurred with a probability of 1.5%,
645 or about 1-2 times per century. Over the next 50 years, such extreme CEs are projected to become almost 10 times more
646 frequent, occurring more than once every 10 years, and reaching much higher temperatures and precipitation deficits.

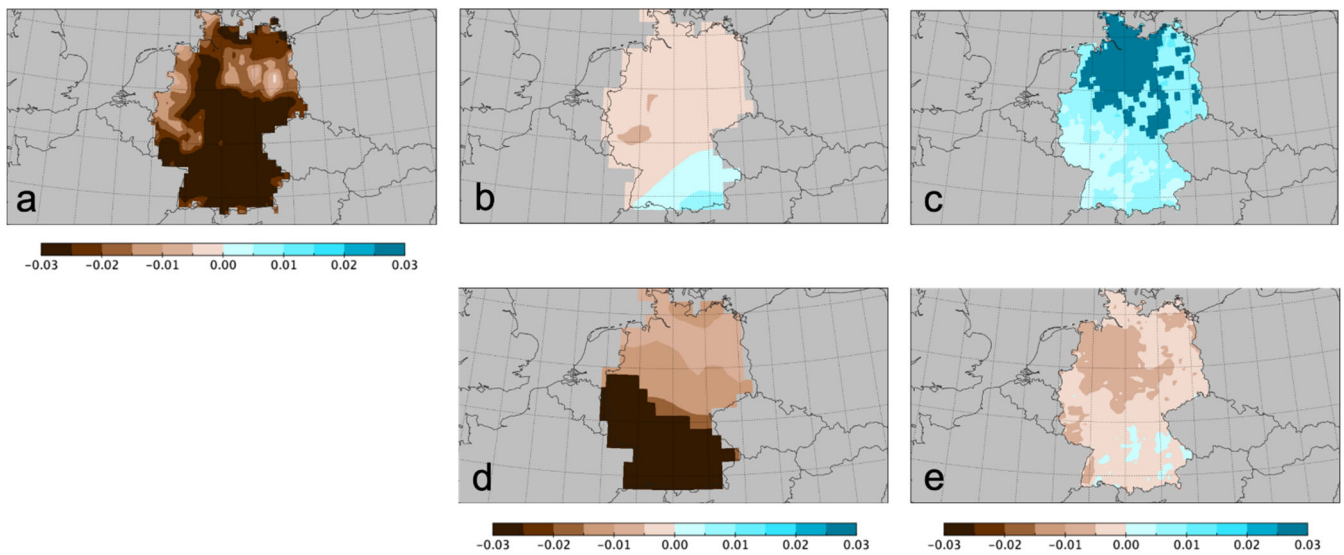


647
648 **Figure 12: Changes of temperature-precipitation (heat-drought, left) and precipitation-wind (wet-windy, right) compound years**
649 **events**-occurrence in terms of frequency and intensity, at 1 °C (1975-2025) and 3 °C (2025-2075) above the pre-industrial levels based
650 **on the 30-member CMIP6 MPI-GE under SSP5_8_5 (Olonscheck et al., 2023) over Germany.**

651
652
653
654
655
656
657
658
659
660
661
662
663
664
665
666
667
668
669
670
671
672
673
674
675
676

The likelihood of winters with extreme compound precipitation-strong wind events does not change significantly with global warming in the CMIP6 MPI-GE projections (Fig. 12, right). Such wet and windy winters, where both precipitation and wind are extreme, are projected to occur about once every 50 years. However, although the number of projected events remains roughly the same, the intensity of the actual wind and precipitation levels reached during the most extreme compound wet-windy events increases substantially in the near future. ~~Moreover, the unprecedented character of the drought conditions of the events in 2018 poses challenges to the ability of climate models to realistically reproduce such conditions.~~

A factor that strongly modulates the occurrence of extremes in Europe is the soil moisture availability, as decreasing soil moisture availability initiates a ~~suitesuit~~ of processes feeding back into an intensification of both heat waves and droughts (Miralles et al., 2019). Figure 13 presents a comparison between the observed (ERA5), simulated (extended historical) and projected (RCP8.5) drought conditions via the SPEI moisture availability index (see Methods section 2.12). For the historical period 1979-2019, the rReanalysis shows trends in the 3-year running mean SPEI, with a clear drying tendency in central and southern Germany during the warm season, with lower values elsewhere in Germany (Fig. 13a). Part of this trend may be related to the multi-year drought of 2018-2020 at the end of the time series. The CMIP5 multi-model ensemble under observed (extended historical) greenhouse gas concentrations (Fig. 13b) fails however at depicting the trends for the past decades, while Euro-CORDEX (Fig. 13c) simulates an increased water availability across Germany. The future projections following the RCP8.5 scenario are roughly consistent between CMIP5 (Fig. 13d) and EURO-CORDEX (Fig. 13e). Both ensembles predict a considerable trend towards more impactful multi-year drought conditions under RCP8.5. Differences between the various sources of data may be related to specific characteristics and settings of the climate models, such as the treatment of anthropogenic aerosols, the inherited uncertainty and bias of climate models to replicate the precipitation variability at the regional and local scale, the differences of the convective precipitation during the warm part of the year (Dyrrdal et al., 2017), but also the use of multi-model ensembles that may mask the individual model skill (Ridder et al., 2022). These examples demonstrate the need for further model development to improve their ability to accurately reproduce observed CEs and their characteristics, thus reducing the uncertainty of future projections and contributing to improved prevention, risk management and future preparedness.



677
 678 **Figure 13: Decadal trends, 1975-2021 and 2022-2077, of the 3-yr running mean Standardized Precipitation Evapotranspiration**
 679 **Index for (a) ERA5, (b) historical CMIP5 multi-model ensemble extended by Aalbers et al. (2023), (c) EURO-CORDEX multi-model**
 680 **ensemble, (d) RCP8.5 CMIP5 multi-model ensemble, and (e) RCP8.5 EURO-CORDEX multi-model ensemble. Significant model**
 681 **ensemble grid points are shaded dark brown and dark green. Units in standard deviation for spring and summer.**

682
 683 **5 Conclusions – Lessons learned and future steps**

684 Compound climate events had severe impacts across Europe in 2018, as combinations of extreme weather events unfolded
 685 simultaneously or in succession, resulting in extensive socio-economic, environmental, and infrastructural damage. The study
 686 highlights two primary types of CEs: hot-dry and wet-windy, each amplifying the effects of individual weather extremes. A
 687 variety of statistical approaches and datasets have been explored and implemented, spanning different types of events and
 688 disciplines.

689 The summer of 2018 was marked by prolonged heatwaves and drought conditions across Europe, driven largely by persistent
 690 large-scale atmospheric blocking. Soil moisture declined sharply from spring through summer, imposing widespread stress on
 691 agriculture, forests, and water resources. These conditions led to significant agricultural losses, particularly in winter wheat
 692 yields, and imposed severe stress on European forests, resulting in large-scale forest fires and insect outbreaks.

693 The winter of 2018 saw a sequence of intense storms, including Friederike and Burglind, which brought strong winds and
 694 heavy precipitation, causing widespread flooding, property damage, and economic losses in multiple countries. The
 695 combination of sustained high winds and heavy precipitation further increased the risk of landslides and rockfalls, particularly
 696 in regions with saturated and thawing soils.

697 Projections indicate that, under progressing climate change, hot-dry events will increase in frequency and severity, while wet-
 698 windy events may retain similar frequencies but with greater intensity. Current adaptation and risk management strategies may

699 be insufficient, as they often focus on single-event risks and may underestimate the compound hazards posed by concurrent
700 extremes.

701 This study encourages further research on compound events to improve predictive capabilities and inform adaptation strategies.
702 Integrated climate models that better represent the complex interactions of multiple extremes are crucial. Next steps involve
703 validating the physical relationships between predictors and CEs to identify the underlying mechanisms that drive or modify
704 these events, which could lead to more accurate analyses and predictions of CEs. Furthermore, given the complexity of CEs
705 and their direct impacts, a redefinition of events based primarily on their relevant impacts, rather than purely statistical
706 characteristics, is necessary to effectively assess and manage these risks.

707 These findings underscore the need for comprehensive climate adaptation approaches that address the interconnected nature
708 of compound events, ensuring more effective preparedness for the compounded risks of future climate extremes.

709 The case studies presented in this paper illustrate the role of CEs for impact studies exemplified with the calendar year of 2018,
710 as an exceptional year of various multi-variate extremes. Our approach follows a user-oriented climate change research path
711 which addresses the socio-economic effects of the meteorological changes (IPCC, 2022). ~~Within climXtreme, a variety of~~
712 statistical approaches and datasets have been explored and implemented. ~~The showcases presented in this paper include~~
713 multivariate, pre-conditioning, temporally and spatial CEs (see Zscheischler et al., 2020; Bevacqua et al., 2021). Combinations
714 of heat and drought stress as well as windstorms, convective storms and heavy precipitation led to unprecedented impacts on
715 ecosystems, infrastructure and societies. These case studies demonstrate science advancements in various aspects and
716 contribute to a better process understanding of CEs, as well as generated new knowledge with respect to better informed risk
717 management (e.g. Toreti et al., 2019; de Brito et al., 2020; Mastrotheodoros et al., 2020; Conradt et al., 2023) enhanced
718 preparedness and resilience against CEs, their consequences and impacts at the German national and European scales.

719 The hot and dry summer of 2018 was characterised by a combination of concurrent meteorological conditions and impacts that
720 amplified each other and led to even larger secondary impacts with unprecedented social, ecological and economic
721 consequences. The heatwaves of summer 2018, prominent events in terms of seasonal variability, were preceded by an intense
722 and persistent drought that began in spring and extended into early summer and autumn. The persistent large scale atmospheric
723 blocking conditions (e.g. Rösner et al., 2019) favoured the occurrence of the heatwaves over central Europe, with hotspot areas
724 coinciding with regions of weak winds between the polar and subtropical jets. The soil moisture deficit that developed in spring
725 and early summer 2018 reached the lowest soil layers with a time lag of about three months, while the intense dryness affected
726 groundwater storage. Taking into account the memory effect of groundwater storage, a full recovery from a drought affecting
727 surface water storage takes longer than one year. A partial recovery of deficits during the winter of 2019 did not reach the
728 lowest soil layers, which were affected anew by the recurrent dry conditions of the following spring and summer. The lack of
729 soil moisture extended to the entire soil column and thus to the entire root zone of the vegetation during both summers of 2018
730 and 2019, placing the vegetation under soil moisture stress. In addition, the ability to use irrigation as a tool to mitigate the
731 agricultural drought was further compromised by the co-occurrence of the agricultural and hydrological droughts. The
732 constellation of climatic anomalies across Europe resulted in an average winter wheat yield loss of 22% compared to the

733 previous 30 years over large areas of Germany. Lastly, the combination of drought and heat stress on trees led to a sharp
734 reduction in green cover, insect outbreaks and an increased risk of forest fires in Europe, with serious environmental, economic
735 and social consequences.

736 The combined influence of strong winds and heavy precipitation, associated with a series of intense storms in the winter of
737 2018, demonstrated the risk and damage characteristics of CEs. Among these, Friederike (David) and Burglind (Eleanor) were
738 connected with strong winds and heavy snowfall that caused extensive damage along their paths across Europe. The assessment
739 of the impact of winter storm Friederike in terms of losses clearly classifies it as a CE, making it the costliest windstorm of the
740 last decade. The analysis of the wind and precipitation variables during the winter storm Friederike showed the extreme nature
741 of the wind, and the long duration of the precipitation, related to the slow movement of the storm. Furthermore, the sequence
742 of the two storms may have amplified the effects of the long precipitation and thaw levels, favouring the rockfall event in
743 Lower Saxony. In the early summer of 2018, the developed atmospheric blocking not only contributed to the occurrence of
744 the heatwaves, but also favoured the occurrence of severe convective storms on the western flank of the block over several
745 days (up to three weeks) with unusually high precipitation. The impact of such persistent convective events increases the risk
746 of flooding and damage, especially following the intense drought in spring 2018 in the area.

747 Our analyses have also shown that both types of CEs may change under future climate conditions both in terms of their
748 frequency and severity. Indeed, future projections indicate an increase in the frequency of many types of extreme events (IPCC,
749 2022), so quantifying the likelihood of future extreme events is becoming increasingly important for adaptation planning.
750 Furthermore, it is critical to accurately examine the links between these types of events, as the risk and return periods of
751 extreme events may be significantly underestimated by assuming the independence of these events, or by examining only a
752 single extreme event. To ensure a coherent risk assessment of high risk events such as CEs, multiple drivers should be
753 considered that play a synergistic and reinforcing role. Further studies aim at expanding the current knowledge on the complex
754 relationships between CEs and large-scale fields at different time horizons in order to improve the detection and thus the
755 understanding of the climate system. The next step would be to validate the physical relationships between predictors and CEs
756 to identify the physical mechanisms that drive or impact these events, which may improve the analysis and potentially the
757 prediction of CEs. Furthermore, given the nature of CEs, their complexity and their direct links to impacts, a definition of
758 events that relies primarily on the relevant impacts prior to their statistical characterisation is required. Considering the
759 uncertainties associated with future projections and the multivariate character of drivers and events, CEs pose major challenges
760 and lead to limitations in the development of effective adaptation strategies, making research in this direction imperative.
761 Therefore, further dedicated research is needed towards a comprehensive view of CEs and their impacts in a warming world.

764 **Code availability**

765 Code is available from the authors upon request.

767 **Data availability**

768 The ERA5 (<https://doi.org/10.1002/qj.3803>, Hersbach et al., 2020) reanalysis data are publicly available via the Copernicus
769 Climate Change Service (<https://doi.org/10.24381/cds.adbb2d47>, Hersbach et al., 2023). The gridded observational datasets
770 E-OBS (<https://doi.org/10.1029/2017JD028200>, Cornes et al., 2018) are publicly available on the European Climate
771 Assessment & Dataset website (<https://www.ecad.eu/download/ensembles/download.php>, ECA&D, 2023). The observational
772 datasets (<https://doi.org/10.5194/asr-10-99-2013>, Kaspar et al., 2013) and the phenological data from the German Weather
773 Service (DWD; <https://doi.org/10.5194/asr-11-93-2014>, Kaspar et al., 2015) are publicly available on the DWD website under
774 their Open Data Portal (<https://opendata.dwd.de/>, DWD, 2023). The yield productivity data (<http://dx.doi.org/10.22029/jlupub-7177>,
775 Ellsäßer and Xoplaki, 2022a), the yield anomaly catalogue (<http://dx.doi.org/10.22029/jlupub-7176>, Ellsäßer and
776 Xoplaki, 2022b) and supplementary data (<http://dx.doi.org/10.22029/jlupub-7203>, Ellsäßer and Xoplaki, 2022c) are publicly
777 available at the JLUpub research data repository. Historic climate data from the GSWP-W5E5 dataset used for LPJmL5
778 simulations are available from <https://doi.org/10.48364/ISIMIP.982724> (Lange et al., 2022). The historical data of atmospheric
779 N deposition and atmospheric CO₂ concentrations can be obtained from <https://doi.org/10.48364/ISIMIP.600567> (Yang and
780 Tian, 2020) and <https://doi.org/10.48364/ISIMIP.664235.2> (Büchner and Reyer, 2022), respectively. All input data, model
781 code, model outputs, and post-processing scripts that have been used to produce the LPJmL-related results in this paper are
782 archived at the Potsdam Institute for Climate Impact Research and are available upon request.

783 **Competing interests**

784 At least one of the (co-)authors is a member of the editorial board of Natural Hazards and Earth System Sciences. The peer-
785 review process was guided by an independent editor, and the authors ~~also have~~ ~~have also~~ no other competing interests to declare.

787 **Author Contribution**

788 EX and FE coordinated the interdisciplinary task force on compound events within climXtreme and this collaborative paper,
789 conducted the agriculture case study analysis with Figure 6, prepared the first and final drafts of the paper based on the
790 contribution of the co-authors; ER contributed the drivers of the hot summer of 2018 case study with Figure 1; SS contributed
791 the detection of spatial patterns of extreme events and Figure 2; LG and SK contributed with the surface water storage case
792 study analysis and Figure 3; LJ contributed the soil moisture case study and Figure 4; JH contributed with the analysis of the
793 agricultural and hydrological droughts and Figure 5; DG and FK contributed with the forestry case study; JGP and T-CC
794 contributed the windstorms description and prepared Figure 7 and S1; JGP contributed to the compound events under climate
795 change section; JG conducted the loss analysis for windstorms with Figure 8 and contributed to the methods section; FS
796 conducted the copula analysis and prepared Figure 9; KNM contributed the rockfall events case study analysis with Figure 10,
797 drafted the section on precipitation-wind compound events and contributed to the compound events under climate change

798 section; SM and MA analysed convective storms and provided Figure 11; LSG did the CMIP6 MPI-GE projection study and
799 prepared Figure 12; KH contributed the analysis of soil moisture representation and trend in model simulations with Figure
800 13. NL and OV contributed to the temperature-precipitation compound events section; JL contributed drafting different
801 sections and versions of the paper and all authors followed the analysis from the beginning, provided text and
802 edited/commented the final version of the manuscript.

803 **Acknowledgements**

804 This paper is a collaborative effort within the BMBF climXtreme project, for which the authors acknowledge funding (grant
805 numbers 01LP1901A, 01LP1903C, 01LP1901F, 01LP1903A, 01LP1902J, 01LP1903F, 01LP1902M, 01LP1901E). EX, NL,
806 OV acknowledge support by the EU Horizon 2020 Project CLINT under Grant Agreement number 101003876. EX
807 acknowledges support by the BMWK project DAKI-FWS (grant number 01MK21009I) and the EU Horizon Europe project
808 MedEWSa under Grant Agreement number 101121192. JGP thanks the AXA research fund for support. LSG has also received
809 funding from the European Union's Horizon Europe Framework Programme under the Marie Skłodowska-Curie grant
810 agreement No 101064940. SMVB acknowledges funding from the DFG training group NatRiskChange (grant No GRK
811 2043/1). We acknowledge the World Climate Research Programme's Working Group on Coupled Modelling, which is
812 responsible for CMIP, and we thank the climate modelling groups for producing and making available their model output. For
813 CMIP the U.S. Department of Energy's Program for Climate Model Diagnosis and Intercomparison provides coordinating
814 support and led development of software infrastructure in partnership with the Global Organization for Earth System Science
815 Portals. We acknowledge the World Climate Research Programme's Working Group on Regional Climate, and the Working
816 Group on Coupled Modelling, former coordinating body of CORDEX and responsible panel for CMIP5. We also thank the
817 climate modelling groups for producing and making available their model output. We also acknowledge the Earth System Grid
818 Federation infrastructure, an international effort led by the U.S. Department of Energy's Program for Climate Model Diagnosis
819 and Intercomparison, the European Network for Earth System Modelling and other partners in the Global Organisation for
820 Earth System Science Portals (GO-ESSP). We acknowledge the E-OBS dataset from the EU-FP6 project UERRA
821 (<http://www.uerra.eu>) and the Copernicus Climate Change Service, and the data providers in the ECA&D project
822 (<https://www.ecad.eu>).

823 **References**

- 824 Aalbers, E. E., van Meijgaard, E., Lenderink, G., de Vries, H., and van den Hurk, B. J. J. M.: The 2018 west-central European
825 drought projected in a warmer climate: how much drier can it get?, *Nat. Hazards Earth Syst. Sci.*, 23, 1921–1946,
826 <https://doi.org/10.5194/nhess-23-1921-2023>, 2023.
- 827 Allen, C. D., Breshears, D. D., and McDowell, N. G.: On underestimation of global vulnerability to tree mortality and forest
828 die-off from hotter drought in the Anthropocene, *Ecosphere*, 6, 1-55, 2015.

- 829 Augenstein, M., Mohr, S., and Kunz, M.: Analysis of thunderstorm clusters derived from lightning data with ST-DBSCAN in
830 West and Central Europe, *Nat. Hazards Earth Syst. Sci.*, in prep.
- 831 Barriopedro, D., Fischer, E.M., Luterbacher, J., Trigo, R.M., and García-Herrera, R.: The hot summer of 2010: redrawing the
832 temperature record map of Europe, *Science*, 332, 220-224, 2011.
- 833 Bastos, A., et al.: Direct and seasonal legacy effects of the 2018 heat wave and drought on European ecosystem productivity,
834 *Sci. Adv.*, 6, eaba2724, <https://doi.org/10.1126/sciadv.aba2724>, 2020.
- 835 Bastos, A., Orth, R., Reichstein, M., Ciais, P., Viovy, N., et al.: Vulnerability of European ecosystems to two compound dry
836 and hot summers in 2018 and 2019, *Earth Syst. Dyn.*, 12:1015–1035, 2021, <https://doi.org/10.5194/esd-12-1015-2021>
- 837 Beloiu, M., Stahlmann, R., and Beierkuhnlein, C.: High Recovery of Saplings after Severe Drought in Temperate Deciduous
838 Forests, *Forests*, 11:546, <https://doi.org/10.3390/f11050546>, 2020.
- 839 Beillouin, D., Schauburger, B., Bastos, A., Ciais, P., and Makowski, D.: Impact of extreme weather conditions on European
840 crop production in 2018, *Philos. T. R. Soc. B*, 375, 20190510, <https://doi.org/10.1098/rstb.2019.0510>, 2020.
- 841 Bender, J.: Zur Ermittlung von hydrologischen Bemessungsgrößen an Flussmündungen mit Verfahren der multivariaten
842 Statistik. Mitteilung des Forschungsinstituts Wasser und Umwelt der Universität Siegen, 9. [http://dokumentix.ub.uni-](http://dokumentix.ub.uni-siegen.de/opus/volltexte/2015/965/pdf/Dissertation_Jens_Bender.pdf)
843 [siegen.de/opus/volltexte/2015/965/pdf/Dissertation_Jens_Bender.pdf](http://dokumentix.ub.uni-siegen.de/opus/volltexte/2015/965/pdf/Dissertation_Jens_Bender.pdf), 2015.
- 844 Bevacqua, E., De Michele, C., Manning, C., Couasnon, A., Ribeiro, A. F. S., Ramos, A. M., et al.: Guidelines for studying
845 diverse types of compound weather and climate events, *Earth's Future*, 9:e2021EF002340,
846 <https://doi.org/10.1029/2021EF002340>, 2021.
- 847 Bevacqua, E., Maraun, D., Hobæk Haff, I., Widmann, M., and Vrac, M.: Multivariate statistical modelling of compound events
848 via pair-copula constructions: analysis of floods in Ravenna (Italy), *Hydrol. Earth Syst. Sci.*, 21, 2701–2723.
849 <https://doi.org/10.5194/hess-21-2701-2017>, 2017.
- 850 Bevacqua, E., Suarez-Gutierrez, L., Jézéquel, A., Lehner, F., Vrac, M., Yiou, P., and Zscheischler J.: Advancing research on
851 compound weather and climate events via large ensemble model simulations, *Nat. Commun.*, 14, 2145,
852 <https://doi.org/10.1038/s41467-023-37847-5>, 2023.
- 853 Birant, D., and Kut, A.: ST-DBSCAN: An algorithm for clustering spatial-temporal data. *Data Know. Eng.*, 60, 208-221,
854 <https://doi.org/10.1016/j.datak.2006.01.013>, 2007.

- 855 [Blauhut, V., Stoelzle, M., Ahopelto, L., Brunner, M. I., Teutschbein, C., Wendt, D. E., Akstinas, V., Bakke, S. J., Barker, L.](#)
856 [J., Bartošová, L., Briede, A., Cammalleri, C., Kalin, K. C., De Stefano, L., Fendeková, M., Finger, D. C., Huysmans, M.,](#)
857 [Ivanov, M., Jaagus, J., Jakubínský, J., Krakovska, S., Laaha, G., Lakatos, M., Manevski, K., Neumann Andersen, M.,](#)
858 [Nikolova, N., Osuch, M., van Oel, P., Radeva, K., Romanowicz, R. J., Toth, E., Trnka, M., Urošev, M., Urquijo Reguera,](#)
859 [J., Sauquet, E., Stevkov, A., Tallaksen, L. M., Trofimova, I., Van Loon, A. F., van Vliet, M. T. H., Vidal, J.-P., Wanders,](#)
860 [N., Werner, M., Willems, P., and Živković, N.: Lessons from the 2018–2019 European droughts: a collective need for](#)
861 [unifying drought risk management, Nat. Hazards Earth Syst. Sci., 22, 2201–2217, \[https://doi.org/10.5194/nhess-22-2201-\]\(https://doi.org/10.5194/nhess-22-2201-2022\)](#)
862 [2022, 2022.](#)
- 863 Brakkee, E., van Huijgevoort, M. H. J., and Bartholomeus, R. P.: Improved understanding of regional groundwater drought
864 development through time series modelling: the 2018–2019 drought in the Netherlands, Hyd. Earth Sys. Sci., 26, 551–569.
865 <https://doi.org/10.5194/hess-26-551-2022>, 2022.
- 866 Brauns, B., Cuba, D., Bloomfield, J. P., Hannah, D. M., Jackson, C., Marchant, B. P., et al.: The Groundwater Drought
867 Initiative (GDI): Analysing and understanding groundwater drought across Europe, Proc. Int. Assoc. Hydrol. Sci., 383,
868 297–305. <https://doi.org/10.5194/piahs-383-297-2020>, 2020.
- 869 Brun, P., Psomas, A., Ginzler, C., Thuiller, W., Zappa, M., and Zimmermann, N. E.: Large-scale early-wilting response of
870 Central European forests to the 2018 extreme drought, Glob. Change Biol., 26, 7021-7035, 2020.
- 871 Büchner, M., and Reyer, C.: ISIMIP3a atmospheric composition input data (v1.2). ISIMIP Repository.
872 <https://doi.org/10.48364/ISIMIP.664235.2>, 2022
- 873 Bundesministerium für Ernährung und Landwirtschaft (BMEL): Ergebnisse der Waldzustandserhebung 2020,
874 [https://www.bmel.de/SharedDocs/Downloads/DE/_Wald/ergebnisse-waldzustandserhebung-](https://www.bmel.de/SharedDocs/Downloads/DE/_Wald/ergebnisse-waldzustandserhebung-2020.html)
875 [2020.html](https://www.bmel.de/SharedDocs/Downloads/DE/Broschueren/ergebnisse-waldzustandserhebung-2020.pdf?__blob=publicationFile&v=11)~~[https://www.bmel.de/SharedDocs/Downloads/DE/Broschueren/ergebnisse-waldzustandserhebung-](https://www.bmel.de/SharedDocs/Downloads/DE/Broschueren/ergebnisse-waldzustandserhebung-2020.pdf?__blob=publicationFile&v=11)~~
876 ~~[2020.pdf?__blob=publicationFile&v=11](https://www.bmel.de/SharedDocs/Downloads/DE/Broschueren/ergebnisse-waldzustandserhebung-2020.pdf?__blob=publicationFile&v=11)~~, 2021, (Accessed ~~19 October~~~~21 June~~20243)
- 877 Buras, A., Rammig, A., and Zang, C. S.: Quantifying impacts of the 2018 drought on European ecosystems in comparison to
878 2003, Biogeosciences, 17, 1655-1672, 2020.
- 879 Caldeira, M.C., Lecomte, X., David, T.S., Pinto, J.G., Bugalho, M.N., and Werner, C.: Synergy of extreme drought and plant
880 invasion reduce ecosystem functioning and resilience. Sci. Reports, 5, 15110 <https://doi.org/10.1038/srep15110>, 2015
- 881 Carnicer, J., Alegria, A., Giannakopoulos, C. et al.: Global warming is shifting the relationships between fire weather and
882 realized fire-induced CO₂ emissions in Europe, Sci. Rep., 12, 10365, <https://doi.org/10.1038/s41598-022-14480-8>, 2022

- 883 Cerlini, P. B., Silvestri, L., Meniconi, S., and Brunone, B.: Simulation of the Water Table Elevation in Shallow Unconfined
884 Aquifers by means of the ERA5 Soil Moisture Dataset: The Umbria Region Case Study, *Earth Inter.*, 25, 15–32.
885 <https://doi.org/10.1175/EI-D-20-0011.1>, 2021.
- 886 Conradt, T., Engelhardt, H., Menz, C. et al.: Cross-sectoral impacts of the 2018–2019 Central European drought and climate
887 resilience in the German part of the Elbe River basin, *Reg. Environ. Change*, 23, [https://doi.org/10.1007/s10113-023-](https://doi.org/10.1007/s10113-023-02032-3)
888 02032-3, 2023.
- 889 Cornes, R.C., van der Schrier, G., van den Besselaar, E.J.M., and Jones, P.D.: An Ensemble Version of the E-OBS Temperature
890 and Precipitation Data Sets, *J. Geophys. Res. Atmospheres* 123, 9391–9409. <https://doi.org/10.1029/2017JD028200>, 2018.
- 891 Cooley, D., and Thibaud, E.: Decompositions of dependence for high-dimensional extremes, *Biometrika*, 106, 587–604, 2019.
- 892 Cucchi, M., Weedon, G. P., Amici, A., Bellouin, N., Lange, S., Müller Schmied, H., Hersbach, H., and Buontempo, C.:
893 WFDE5: bias-adjusted ERA5 reanalysis data for impact studies, *Earth Sys. Sci. Data*, 12, 2097–2120.
894 <https://doi.org/10.5194/essd-12-2097-2020>, 2020.
- 895 Di Capua, G., Sparrow, S., Kornhuber, K., Rousi, E., Osprey, S., Wallom, D., van den Hurk, B. and Coumou, D.: Drivers
896 behind the summer 2010 wave train leading to Russian heatwave and Pakistan flooding, *npj Clim. Atmos. Sci.*, 4, 55,
897 <https://doi.org/10.1038/s41612-021-00211-9>, 2021.
- 898 D’Agostino, V.: Drought in Europe summer 2018: Crisis management in an orderly chaos, *Farm-Europe*, [https://www.farm-](https://www.farm-europe.eu/blog-en/drought-in-europe-summer-2018-crisis-management-in-an-orderly-chaos/)
899 [europe.eu/blog-en/drought-in-europe-summer-2018-crisis-management-in-an-orderly-chaos/](https://www.farm-europe.eu/blog-en/drought-in-europe-summer-2018-crisis-management-in-an-orderly-chaos/), 2018, (Accessed 19 October
900 21 June 2024).
- 901 D’Amato, J., Hantz, D., Guerin, A., Jaboyedoff, M., Baillet, L., and Mariscal, A.: Influence of meteorological factors on
902 rockfall occurrence in a middle mountain limestone cliff, *Nat. Hazards Earth Syst. Sci.*, 16, 719–735,
903 <https://doi.org/10.5194/nhess-16-719-2016>, 2016.
- 904 Dacre, H.F., Hawcroft, M.K., Stringer, M.A. and Hodges, K.I.: An extratropical cyclone database: A tool for illustrating
905 cyclone structure and evolution characteristics, *Bull. Amer. Meteorol. Soc.*, 93, 1497–1502, [https://doi.org/10.1175/BAMS-](https://doi.org/10.1175/BAMS-D-11-00164.1)
906 [D-11-00164.1](https://doi.org/10.1175/BAMS-D-11-00164.1), 2012.
- 907 de Brito, M., Kuhlicke, C. and Marx, A.: Near-real-time drought impact assessment: a text mining approach on the 2018/19
908 drought in Germany, *Environ. Res. Lett.*, 15, 1040a9, 2020.

- 909 Drouard, M., Kornhuber, K., and Woollings, T.: Disentangling dynamic contributions to summer 2018 anomalous weather
910 over Europe, *Geophys. Res. Lett.*, 46, 12537–12546, 2019.
- 911 Dyrørdal, A.V., Stordal, F., Lussana, C.: Evaluation of summer precipitation from EURO-CORDEX fine-scale RCM
912 simulations over Norway, *Int. J. Clim.*, 38, 1661-1677, <https://doi.org/10.1002/joc.5287>, 2017
- 913 Eisenstein, L., Schulz, B., Qadir, G. A., Pinto, J. G. and Knippertz, P.: Identification of high-wind features within extratropical
914 cyclones using a probabilistic random forest – Part 1: Method and case studies, *Weather Clim. Dynam.*, 3, 1157–1182,
915 <https://doi.org/10.5194/wcd-3-1157-2022>, 2022.
- 916 Ellsäßer, F. and Xoplaki, E.: Cropdata – spatial yield productivity data base for the ten most cultivated crops in Germany from
917 1989 to 2020 - version 1.0. <http://dx.doi.org/10.22029/jlupub-7177>, 2022a.
- 918 Ellsäßer, F. and Xoplaki, E.: Cropdata – yield anomaly catalogue for the ten most cultivated crops in Germany from 1989 to
919 2020 - version 1.0. <http://dx.doi.org/10.22029/jlupub-7176>, 2022b.
- 920 Ellsäßer, F. and Xoplaki, E.: Cropdata – supplementary data (for spatial yield productivity data base for the ten most cultivated
921 crops in Germany from 1989 to 2020) - version 1.0. <http://dx.doi.org/10.22029/jlupub-7203>, 2022c.
- 922 Ellsäßer, F. and Xoplaki, E. (in review): A unique high-resolution open access crop yield database for Germany covering the
923 period 1989 to 2020, *Scientific Data*, 2024.
- 924 Ester, M., Kriegel, H.P. Sander, J., Xu, X., Simoudis, E., Han, J., and Fayyad, U.M. (eds.): A density-based algorithm for
925 discovering clusters in large spatial databases with noise. *Proceedings of the Second International Conference on*
926 *Knowledge Discovery and Data Mining (KDD-96)*. AAAI Press. pp. 226–231. CiteSeerX 10.1.1.121.9220. ISBN 1-57735-
927 004-9, 1996
- 928 Feurdean, A., Vannière, B., Finsinger, W., Warren, D., Connor, S.C., Forrest, M., Liakka, J., et al.: Fire hazard modulation by
929 long-term dynamics in land cover and dominant forest type in eastern and central Europe, *Biogeosciences*, 17, 1213–1230,
930 2020.
- 931 Fischer, E. M., Seneviratne, S. I., Vidale, P. L., Lüthi, D., and Schär, C.: Soil moisture—atmosphere interactions during the
932 2003 European summer heatwave, *J. Clim.*, 20: 5081–5099, 2007.
- 933 Fischer, E. M., and Schär, C.: Consistent geographical patterns of changes in high-impact European heatwaves, *Nat. Geosci.*,
934 3, 398–403, <https://doi.org/10.1038/ngeo866>, 2010.

- 935 Fink, A. H., Brücher, T., Krüger, A., Leckebusch, G. C., Pinto, J. G. and Ulbrich, U.: The 2003 European summer heatwaves
936 and drought –synoptic diagnosis and impacts, *Weather*, 59, 209–216, <https://doi.org/10.1256/wea.73.04>, 2004.
- 937 Fink, A. H., Brücher, T., Ermert, V., Krüger, A., and Pinto, J. G.: The European storm Kyrill in January 2007: synoptic
938 evolution, meteorological impacts and some considerations with respect to climate change, *Nat. Hazards Earth Syst. Sci.*,
939 9, 405–423, <https://doi.org/10.5194/nhess-9-405-2009>, 2009.
- 940 Frank, M.J.: On the simultaneous associativity of $F(x,y)$ and $x+y-F(x,y)$, *Aequationes Mathematicae*, 19, 194-226, 1979.
- 941 Furusho-Percot, C., Goergen, K., Hartick, C., Kulkarni, K., Keune, J., and Kollet, S.: Pan-European groundwater to atmosphere
942 terrestrial systems climatology from a physically consistent simulation, *Sci. Data.*, 6. [https://doi.org/10.1038/s41597-019-](https://doi.org/10.1038/s41597-019-0328-7)
943 0328-7, 2019.
- 944 García-Herrera, R., Díaz, J., Trigo, R.M., Luterbacher, J., and Fischer, E. M.: A Review of the European Summer Heat Wave
945 of 2003, *Crit. Rev. Env. Sci. Tech.*, 40, 267-306, <https://doi.org/10.1080/10643380802238137>, 2010.
- 946 Giorgi, F., Jones, C., and Arsar, G. R.: Addressing climate information needs at the regional level: the CORDEX framework,
947 *WMO Bulletin*, 58, 175-183, 2009.
- 948 Hari, V., Rakovec, O., Markonis, Y., Hanel, M., and Kumar, R.: Increased future occurrences of the exceptional 2018–2019
949 Central European drought under global warming, *Sci. Rep.*, 10, 1-10, 2020.
- 950 Hartick, C., Furusho-Percot, C., Goergen, K., & Kollet, S.: An interannual probabilistic assessment of subsurface water storage
951 over Europe, using a fully coupled terrestrial model, *Wat. Res. Res.*, 57, e2020WR027828, 2021.
- 952 Hersbach, H., and Coauthors: The ERA5 global reanalysis, *Q.J.R. Meteorol. Soc.*, 146, 1999-2049,
953 <https://doi.org/10.1002/qj.3803>, 2020.
- 954 Hersbach, H., Bell, B., Berrisford, P., Biavati, G., Horányi, A., Muñoz Sabater, J., Nicolas, J., Peubey, C., Radu, R., Rozum,
955 I., Schepers, D., Simmons, A., Soci, C., Dee, D., and Thépaut, J-N.: ERA5 hourly data on single levels from 1940 to
956 present. Copernicus Climate Change Service (C3S) Climate Data Store (CDS), <https://doi.org/10.24381/cds.adbb2d47>,
957 2023, (~~Accessed 19 October 23 June 2024~~).
- 958 Hlásny, T., Zimová, S., Merganičová, K., Štěpánek, P., Modlinger, R., and Turčáni, M: Devastating outbreak of bark beetles
959 in the Czech Republic: Drivers, impacts, and management implications, *For. Ecol. Manage.*, 490,
960 <https://doi.org/10.1016/j.foreco.2021.119075>, 2021.

- 961 Herzfeld, T., Heinke, J., Rolinski, S., and Müller, C.: Soil organic carbon dynamics from agricultural management practices
962 under climate change, *Earth Sys. Dyn.*, 12, 1037–1055, <https://doi.org/10.5194/esd-12-1037-2021>, 2021.
- 963 IPCC: Impacts, Adaptation, and Vulnerability. Contribution of Working Group II to the Sixth Assessment Report of the
964 Intergovernmental Panel on Climate Change [H.-O. Pörtner, D.C. Roberts, M. Tignor, E.S. Poloczanska, K. Mintenbeck,
965 A. Alegría, M. Craig, S. Langsdorf, S. Löschke, V. Möller, A. Okem, B. Rama (eds.)]. Cambridge University Press.
966 Cambridge University Press, Cambridge, UK and New York, NY, USA, 3056 pp., <https://doi.org/10.1017/9781009325844>,
967 2022
- 968 Jane, R., Cadavid, L., Obeysekera, J., Wahl, T.: Multivariate statistical modelling of the drivers of compound flood events in
969 south Florida. *Nat. Hazards Earth Syst. Sci.* 20, 2681–2699, <https://doi.org/10.5194/nhess-20-2681-2020>, 2020
- 970 Kaiser, D., Voynova, Y.G., and Brix, H.: Effects of the 2018 European heatwave and drought on coastal biogeochemistry in
971 the German Bight, *Sci. Tot. Environ.*, 892, 164316, <https://doi.org/10.1016/j.scitotenv.2023.164316>, 2023
- 972 Kaspar, F., Friedrich, K., and Imbery, F.: Observed temperature trends in Germany: Current status and communication tools,
973 *Meteorol. Z. (Contrib. Atm. Sci.)*, <https://doi.org/10.1127/metz/2023/1150><https://doi.org/10.1127/metz/2023/1150>, 2023.
- 974 Kaspar, F., Müller-Westermeier, G., Penda, E., Mächel, H., Zimmermann, K., Kaiser-Weiss, A., and Deutschländer, T.:
975 Monitoring of climate change in Germany – data, products and services of Germany’s National Climate Data Centre, *Adv.*
976 *Sci. Res.*, 10, 99–106, <https://doi.org/10.5194/asr-10-99-2013>, 2013.
- 977 Kaspar, F., Zimmermann, K., and Polte-Rudolf, C.: An overview of the phenological observation network and the phenological
978 database of Germany’s national meteorological service (Deutscher Wetterdienst), *Adv. Sci. Res.*, 11, 93–99, 2015.
- 979 Kautz, L.A., Martius, O., Pfahl, S., Pinto, J.G., Ramos, A.M., Sousa, P.M., and Woollings, T.: Atmospheric Blocking and
980 Weather Extremes over the Euro-Atlantic Sector - A Review, *Weather Clim. Dynam.* 3, 305-336,
981 <https://doi.org/10.5194/wcd-3-305-2022>, 2022
- 982 Kendall, M.G.: Rank correlation methods. 4 ed., 2. Impr. London: Griffin. ISBN 0852641990, 1975.
- 983 Kim, H.: Global Soil Wetness Project Phase 3 Atmospheric Boundary Conditions (Experiment 1) [Data set]. Data Integration
984 and Analysis System (DIAS), <https://doi.org/10.20783/DIAS.501>, 2017.
- 985 Kohonen, T.: Essentials of the self-organizing map, *Neural Networks*, 37, 52–65,
986 <https://doi.org/10.1016/j.neunet.2012.09.018>, 2013.

- 987 Kornhuber, K., Osprey, S., Coumou, D., Petri, S., Petoukhov, V., Rahmstorf, S. and Gray, L.: Extreme weather events in early
988 Summer 2018 connected by a recurrent hemispheric wave pattern, *Environ. Res. Lett.*, 14, 054002,
989 <https://doi.org/10.31223/osf.io/tq23m>, 2019.
- 990 Kornhuber, K., Coumou, D., Vogel, E., Lesk, C., Donges, J. F., Lehmann, J. and Horton, R. M.: Amplified Rossby waves
991 enhance risk of concurrent heatwaves in major breadbasket regions, *Nat. Clim. Chang.*, 10, 48–53,
992 <https://doi.org/10.1038/s41558-019-0637-z>, 2020.
- 993 Lange, S., Mengel, M., Treu, S., and Büchner, M.: ISIMIP3a atmospheric climate input data (v1.0), ISIMIP Repository,
994 <https://doi.org/10.48364/ISIMIP.982724>, 2022.
- 995 Leonard, M., Westra, S., Phatak, A., Lambert, M., van den Hurk, B., McInnes, K., Risbey, J., Schuster, S., Jakob, D., and
996 Stafford-Smith, M.: A compound event framework for understanding extreme impacts, *WIREs. Clim. Change*, 5, 113–
997 128, <https://doi.org/10.1002/wcc.252>, 2014.
- 998 Leuschner, C.: Drought response of European beech (*Fagus sylvatica* L.) – a review, *Persp. Plant Ecol., Evol. and Syst.*, 47,
999 125576, <https://doi.org/10.1016/j.ppees.2020.125576>, 2020.
- 1000 Lidskog, R., Johansson, J., and Sjödin, D.: Wildfires, responsibility and trust: public understanding of Sweden’s largest wildfire,
1001 *Scand. J. For. Res.*, 34, 319–328, 2019.
- 1002 Liu, Xuebang, et al.: Similarities and differences in the mechanisms causing the European summer heatwaves in 2003, 2010,
1003 and 2018, *Earth’s Future*, 7, e2019EF001386, <https://doi.org/10.1029/2019EF001386>, 2020.
- 1004 Lorenz, R., Jaeger, E. B., and Seneviratne, S. I.: Persistence of heat waves and its link to soil moisture memory, *Geophys. Res.*
1005 *Lett.*, 37, L09703, 2010.
- 1006 Lutz, F., Herzfeld, T., Heinke, J., Rolinski, S., Schaphoff, S., von Bloh, W., Stoorvogel, J. J. J., and Müller, C.: Simulating the
1007 effect of tillage practices with the global ecosystem model LPJmL (version 5.0-tillage), *Geosci. Mod. Develop.*, 12, 2419–
1008 2440. <https://doi.org/10.5194/gmd-12-2419-2019>, 2019.
- 1009 Luterbacher, J., Dietrich, D., Xoplaki, E., Grosjean, M. and Wanner, H.: European seasonal and annual temperature variability,
1010 trends and extremes since 1500, *Science*, 303: 1499–1503, 2004.
- 1011 Manning, C., Widmann, M., Bevacqua, E., Van Loon, A. F., Maraun, D., and Vrac, M.: Soil moisture drought in Europe: a
1012 compound event of precipitation and potential evapotranspiration on multiple time scales, *J. Hydrometeorol.*, 19, 1255–
1013 1271, <https://doi.org/10.1175/JHM-D-18-0017.1>, 2018.

- 1014 Manning, C., Widmann, M., Maraun, D., Van Loon, A. F., and Bevacqua, E.: Large spread in the representation of compound
1015 long-duration dry and hot spells over Europe in CMIP5, *Weather Clim. Dynam.*, 4, 309–329, [https://doi.org/10.5194/wcd-](https://doi.org/10.5194/wcd-4-309-2023)
1016 [4-309-2023](https://doi.org/10.5194/wcd-4-309-2023), 2023.
- 1017 Matzarakis, A., Laschewski, G., and Muthers, S.: The Heat Health Warning System in Germany—Application and Warnings
1018 for 2005 to 2019, *Atmosphere*, 11, 170, <https://doi.org/10.3390/atmos11020170>, 2020.
- 1019 McKee, T. B., Doesken, N. J., and Kleist, J.: The relationship of drought frequency and duration to time scales, Eighth
1020 Conference on Appl. Climatol., 179–184, 1993.
- 1021 [Manning, C., Kendon, E.J., Fowler, H.J., Catto, J.F., Chan, S.C., and Sansom, P.G.: Compound wind and rainfall extremes:
1022 Drivers and future changes over the UK and Ireland, *Wea. and Clim. Extremes*, 44, 100673,
1023 <https://doi.org/10.1016/j.wace.2024.100673>, 2024](#)
- 1024 Martius, O.; Pfahl, S. and Chevalier, C.: A global quantification of compound precipitation and wind extremes, *Geophys. Res.
1025 Lett.*, 43, 7709–7717, <https://doi.org/10.1002/2016GL070017>, 2016.
- 1026 [Mastrotheodoros, T., et al.: More green and less blue water in the Alps during warmer summers, *Nat. Clim. Change*, 10, 155–
1027 61, 2020.](#)
- 1028 Messmer, M. and Simmonds, I.: Global analysis of cyclone-induced compound precipitation and wind extreme events, *Weath.
1029 Clim. Extremes*, 32, 100324, 2021.
- 1030 Milanovic, S., Markovic, N., Pamucar, D., Gigovic, L., Kostic, P. and Milanovic, S.D.: Forest Fire Probability Mapping in
1031 Eastern Serbia: Logistic Regression versus Random Forest Method, *Forests*. 12: 5, <https://doi.org/10.3390/fl2010005>,
1032 2021.
- 1033 Miralles, D.G., Gentine, P., Seneviratne, S.I. and Teuling, A.J.: Land–atmospheric feedbacks during droughts and heatwaves:
1034 state of the science and current challenges, *Ann. N.Y. Acad. Sci.*, 1436: 19-35, <https://doi.org/10.1111/nyas.13912>, 2019
- 1035 Mohr, S., Wandel, J., Lenggenhager, S., and Martius, O.: Relationship between atmospheric blocking and warm season
1036 thunderstorms over western and central Europe, *Q. J. Roy. Meteor. Soc.*, 145, 3040–3056, <https://doi.org/10.1002/qj.3603>,
1037 2019.
- 1038 Mohr, S., Wilhelm, J., Wandel, J., Kunz, M., Portmann, R., Punge, H. J., Schmidberger, M., Quinting, J. F., and Grams, C.:
1039 The role of large-scale dynamics in an exceptional sequence of severe thunderstorms in Europe May/June 2018, *Weather
1040 Clim. Dynam.*, 1, 325–348, <https://doi.org/10.5194/wcd-1-325-2020>, 2020.

- 1041 [Deutscher Wetterdienst, 2018: Monatlicher Klimastatus Deutschland August 2018. DWD, Geschäftsbereich Klima und](#)
1042 [Umwelt, Offenbach, 29 Seiten, www.dwd.de/DE/derdwd/bibliothek/fachpublikationen/selbstverlag/selbstverlag_node.](#)
1043 [html \(Accessed: 19th October 2024\).](#)
- 1044 Munich RE, Extreme storms, wildfires and droughts cause heavy nat cat losses in 2018. 08/01/2019 Media Information,
1045 available at: [https://www.munichre.com/en/company/media-relations/media-information-and-corporate-news/media-](https://www.munichre.com/en/company/media-relations/media-information-and-corporate-news/media-information/2019/2019-01-08-media-information.html)
1046 [information/2019/2019-01-08-media-information.html](https://www.munichre.com/en/company/media-relations/media-information-and-corporate-news/media-information/2019/2019-01-08-media-information.html), 2019.
- 1047 Naturgefahrenreport 2019, Die Schaden-Chronik der deutschen Versicherer, Gesamtverband der Deutschen
1048 Versicherungswirtschaft, 56 pages e. V.,
1049 [https://www.gdv.de/resource/blob/51710/e5eaa53a9ec21fb9241120c1d1850483/naturgefahrenreport-2019-schaden-](https://www.gdv.de/resource/blob/51710/e5eaa53a9ec21fb9241120c1d1850483/naturgefahrenreport-2019-schaden-chronik-data.pdf)
1050 [chronik-data.pdf](https://www.gdv.de/resource/blob/51710/e5eaa53a9ec21fb9241120c1d1850483/naturgefahrenreport-2019-schaden-chronik-data.pdf) (Accessed 19 October 2024).
- 1051 Nissen, K. M., Rupp, S., Kreuzer, T. M., Guse, B., Damm, B., and Ulbrich, U.: Quantification of meteorological conditions
1052 for rockfall triggers in Germany, *Nat. Hazards Earth Syst. Sci.*, 22, 2117–2130, [https://doi.org/10.5194/nhess-22-2117-](https://doi.org/10.5194/nhess-22-2117-2022)
1053 [2022](https://doi.org/10.5194/nhess-22-2117-2022), 2022.
- 1054 Nogueira, M.: Inter-comparison of ERA-5, ERA-Interim and GPCP rainfall over the last 40 years: process-based analysis of
1055 systematic and random differences, *J. Hydrol.*, 583, 124632, <https://doi.org/10.1016/j.jhydrol.2020.124632>, 2020.
- 1056 OECD.: *Managing Climate Risks, Facing up to Losses and Damages*, OECD Publishing, Paris,
1057 <https://doi.org/10.1787/55ea1cc9-en>, 2021.
- 1058 Öhrn, P., Berlin, M., Elfstrand, M., Krokene, P., and Jönsson, A. M.: Seasonal variation in Norway spruce response to
1059 inoculation with bark beetle-associated bluestain fungi one year after a severe drought, *For. Ecol. Manage.*, 496, 119443,
1060 2021.
- 1061 Olonscheck, D., Suarez-Gutierrez, L., Milinski, S., et al.: The new Max Planck Institute Grand Ensemble with CMIP6 forcing
1062 and high-frequency model output, *Authorea*, <https://doi.org/10.22541/essoar.168319746.64037439/v1>, May 4, 2023.
- 1063 Orth, R., and Seneviratne, S. I.: Analysis of soil moisture memory from observations in Europe, *J. Geophys. Res.*, 117, D15115,
1064 <https://doi.org/10.1029/2011JD017366>, 2012.
- 1065 Pinto, J. G., Spanghel, T., Ulbrich, U., and P. Speth, P.: Sensitivities of a cyclone detection and tracking algorithm: individual
1066 tracks and climatology, *Met. Zeitschrift*, 14, 823 – 838, <https://doi.org/10.1127/0941-2948/2005/0068>, 2005.

- 1067 Pinto, J.G., Zacharias, S., Fink, A.H., Leckebusch, G.C, and Ulbrich, U.: Factors contributing to the development of extreme
1068 North Atlantic cyclones and their relationship with the NAO, *Clim. Dynam.*, 32, 711–737, <https://doi.org/10.1007/s00382->
1069 008-0396-4, 2009.
- 1070 Piper, D., Kunz, M., Ehmele, F., Mohr, S., Mühr, B., Kron, A., and Daniell, J.: Exceptional sequence of severe thunderstorms
1071 and related flash floods in May and June 2016 in Germany – Part 1: Meteorological background, *Nat. Hazards Earth Syst.*
1072 *Sci.*, 16, 2835–2850, <https://doi.org/10.5194/nhess-16-2835-2016>, 2016.
- 1073 Piper, D. A., Kunz, M., Allen, J. T., and Mohr, S.: Investigation of the temporal variability of thunderstorms in Central and
1074 Western Europe and the relation to large-scale flow and teleconnection patterns, *Q. J. Roy. Meteor. Soc.*, 145, 3644–3666,
1075 <https://doi.org/10.1002/qj.3647>, 2019.
- 1076 Rauthe, M., Steiner, H., Riediger, U., Mazurkiewicz, A., and Gratzki, A.: A Central European precipitation climatology – Part
1077 I: Generation and validation of a high-resolution gridded daily data set (HYRAS), *Meteorol. Z.*, 22, 235–256,
1078 <https://doi.org/10.1127/0941-2948/2013/0436>, 2013.
- 1079 Raymond, C., Horton, R.M., Zscheischler, J., Martius, O., AghaKouchak, A., Balch, J., Bowen, S. G., Camargo, S. J., Hess,
1080 J., Kornhuber, K., Oppenheimer, M., Ruane, A. C., Wahl, T., and White, K.: Understanding and managing connected
1081 extreme events, *Nat. Clim. Chang.*, 10, 611–621, <https://doi.org/10.1038/s41558-020-0790-4>, 2020.
- 1082 Resnick, S. I.: *Heavy-tail phenomena: probabilistic and statistical modelling*, Springer Science & Business Media, 2007.
- 1083 Riahi, K., van Vuuren, D.P., et al.: The Shared Socioeconomic Pathways and their energy, land use, and greenhouse gas
1084 emissions implications: An overview, *Glob. Environ. Change*, 42, 153-168,
1085 <https://doi.org/10.1016/j.gloenvcha.2016.05.009>, 2017.
- 1086 Ridder, N., Pitman, A. J., Westra, S., Ukkola, A., Do, H., Bador, M., et al.: Global hotspots for the occurrence of compound
1087 events, *Nat. Comm.*, 11, 5956, <https://doi.org/10.1038/s41467-020-19639-3>, 2020.
- 1088 Ridder, N. N., Pitman, A. J., & Ukkola, A. M.: Do CMIP6 climate models simulate global or regional compound events
1089 skillfully?, *Geophys. Res. Lett.* 48, e2020GL091152, <https://doi.org/10.1029/2020GL091152>, 2021.
- 1090 Ridder, N.N., Ukkola, A.M., Pitman, A.J. et al.: Increased occurrence of high impact compound events under climate change,
1091 *npj Clim. Atmos. Sci.*, 5, 3, <https://doi.org/10.1038/s41612-021-00224-4>, 2022.
- 1092 [Rösner, B. et al., The long heat wave and drought in Europe in 2018 \[in “State of the Climate in 2018”\], *Bull. Am. Meteorol.*](#)
1093 [Soc.](#), 100, S222–S223, <https://doi.org/10.1175/2019BAMSSStateoftheClimate.1>, 2019

- 1094 Rupp S. and Damm, B.: A national rockfall dataset as a tool for analysing the spatial and temporal rockfall occurrence in
1095 Germany, *Earth Surf. Process. Landforms*, 45, 1528–1538, <https://doi.org/10.1002/esp.4827>, 2020.
- 1096 Rousi, E., Anagnostopoulou, C., Tolika, K. and Maheras, P.: Representing teleconnection patterns over Europe: A comparison
1097 of SOM and PCA methods, *Atmos. Res.*, 152, 123–137, <https://doi.org/10.1016/j.atmosres.2013.11.010>, 2015.
- 1098 Rousi, E., Kornhuber, K., Beobide-Arsuaga, G. et al.: Accelerated western European heatwave trends linked to more-persistent
1099 double jets over Eurasia, *Nat. Commun.*, 13, 3851, <https://doi.org/10.1038/s41467-022-31432-y>, 2022.
- 1100 Rousi, E., Fink, A. H., Andersen, L. S., Becker, F. N., Beobide-Arsuaga, G., Breil, M., Cozzi, G., Heinke, J., Jach, L.,
1101 Niermann, D., Petrovic, D., Richling, A., Riebold, J., Steidl, S., Suarez-Gutierrez, L., Tradowsky, J. S., Coumou, D.,
1102 Düsterhus, A., Ellsäßer, F., Fragkoulidis, G., Gliksman, D., Handorf, D., Haustein, K., Kornhuber, K., Kunstmann, H.,
1103 Pinto, J. G., Warrach-Sagi, K., and Xoplaki, E.: The extremely hot and dry 2018 summer in central and northern Europe
1104 from a multi-faceted weather and climate perspective, *Nat. Hazards Earth Syst. Sci.*, 23, 1699–1718,
1105 <https://doi.org/10.5194/nhess-23-1699-2023>, 2023.
- 1106 Schaphoff, S., von Bloh, W., Rammig, A., Thonicke, K., Biemans, H., Forkel, M., Gerten, D., Heinke, J., Jägermeyr, J.,
1107 Knauer, J., Langerwisch, F., Lucht, W., Müller, C., Rolinski, S., Waha, K., Knauer, J., von Bloh, W., Gerten, D., Jägermeyr,
1108 J., and Waha, K.: LPJmL4 – a dynamic global vegetation model with managed land – Part 1: Model description, *Geosci.
1109 Mod. Develop.* 11, 1343–1375, <https://doi.org/10.5194/gmd-11-1343-2018>, 2018.
- 1110 Schuldt, B., Knutzen, F., Delzon, S., Jansen, S., Müller-Haubold, H., Burrett, R., and Leuschner, C.: How adaptable is the
1111 hydraulic system of European beech in the face of climate change-related precipitation reduction?, *New Phytol.*, 210, 443-
1112 458, 2016.
- 1113 Schuldt, B., Buras, A., Arend, M., Vitasse, Y., Beierkuhnlein, C., Damm, A., and Kahmen, A.: A first assessment of the impact
1114 of the extreme 2018 summer drought on Central European forests, *Basic Appl. Ecol.* 45, 86-103, 2020.
- 1115 Schulz, W., Diendorfer, G., Pedeboy, S., and Poelman, D.R.: The European lightning location system EUCLID – Part 1:
1116 Performance analysis and validation, *Nat. Hazards Earth Syst. Sci.*, 16, 595–605, [https://doi.org/10.5194/nhess-16-595-](https://doi.org/10.5194/nhess-16-595-2016)
1117 2016, 2016.
- 1118 Seneviratne, S. I., et al.: Changes in climate extremes and their impacts on the natural physical environment. *Managing the
1119 Risks of Extreme Events and Disasters to Advance Climate Change Adaptation*, C. B. Field et al., Eds., Cambridge
1120 University Press, 109–230, 2012.

- 1121 Seneviratne, S.I., et al.: The Physical Science Basis. Contribution of Working Group I to the Sixth Assessment Report of the
 1122 Intergovernmental Panel on Climate Change [Masson-Delmotte, V., P. Zhai, A. Pirani, S.L. Connors, C. Péan, S. Berger,
 1123 N. Caud, Y. Chen, L. Goldfarb, M.I. Gomis, M. Huang, K. Leitzell, E. Lonnoy, J.B.R. Matthews, T.K. Maycock, T.
 1124 Waterfield, O. Yelekçi, R. Yu, and B. Zhou (eds.)]. Cambridge University Press, Cambridge, United Kingdom and New
 1125 York, NY, USA, pp. 1513–1766, <https://doi.org/10.1017/9781009157896.013>, 2021.
- 1126 Senf, C., and Seidl, R.: Persistent impacts of the 2018 drought on forest disturbance regimes in Europe, *Biogeosci.*, 18, 5223-
 1127 5230, 2021.
- 1128 [Shyrokaya, A. et al.: Significant relationships between drought indicators and impacts for the 2018–2019 drought in
 1129 Germany, *Environ. Res. Lett.* 19 014037, 2024, DOI 10.1088/1748-9326/ad10d9](#)
- 1130 Simpson, N.P., et al.: A framework for complex climate change risk assessment, *One Earth*, 4, 489–501,
 1131 <https://doi.org/10.1016/j.oneear.2021.03.005>, 2021.
- 1132 Statistische Ämter des Bundes und der Länder. Regionaldatenbank Deutschland,
 1133 <https://www.regionalstatistik.de/genesis/online/logon>, 2021 (Accessed ~~19³ October~~ ~~July 2024~~ ~~43, 2021~~).
- 1134 Song, Y.M., Wang, Z.F., Qi, L.L., and Huang, A.N.: Soil Moisture Memory and Its Effect on the Surface Water and Heat
 1135 Fluxes on Seasonal and Interannual Time Scales, *J. Geophys. Res. Atmos.*, 124, 10730–10741, 2019.
- 1136 Sousa, P. M., et al.: Distinct influences of large-scale circulation and regional feedbacks in two exceptional 2019 European
 1137 heatwaves, *Commun. Earth Environ.*, 1, 48, <https://doi.org/10.1038/s43247-020-00048-9>, 2020.
- 1138 Spensberger, C., Madonna, E., Boettcher, M., Grams, C. M., Papritz, L., Quinting, J. F., Röthlisberger, M., Sprenger, M. and
 1139 Zschenderlein, P.: Dynamics of concurrent and sequential Central European and Scandinavian heatwaves, *Q. J. R.
 1140 Meteorol. Soc.*, 146, 2998–3013, <https://doi.org/10.1002/QJ.3822>, 2020.
- 1141 Stefanon, M., D’Andrea, F. and Drobinski, P.: Heatwave classification over Europe and the Mediterranean region, *Environ.
 1142 Res. Lett.*, 7, 014023, <https://doi.org/10.1088/1748-9326/7/1/014023>, 2012.
- 1143 ~~Szemkus S., and Friederichs, P. (in review): Spatial patterns and indices for heatwave and droughts over Europe using a
 1144 decomposition of extremal dependency, 2023~~
- 1145 [Szemkus S., and Friederichs P.: “Spatial patterns and indices for heat waves and droughts over Europe using a decomposition
 1146 of extremal dependency”. *Advances in Statistical Climatology, Meteorology and Oceanography* 10.1,
 1147 <https://doi.org/10.5194/ascmo-10-29-2024>, 2024.](#)

- 1148 Taylor, K.E., Stouffer, R.J., and Meehl, G.A.: An Overview of CMIP5 and the experiment design, *Bull. Amer. Meteor. Soc.*,
1149 93, 485–498, <https://doi.org/10.1175/BAMS-D-11-00094.1>, 2012.
- 1150 Tjeldeman, E., and Menzel, L.: The development and persistence of soil moisture stress during drought across southwestern
1151 Germany, *Hydrol. and Earth Sys. Sci.*, 25, 2009–2025, <https://doi.org/10.5194/hess-25-2009-2021>, 2021.
- 1152 Toreti, A., Belward, A., Perez-Dominguez, I., Naumann, G., Luterbacher, J., Cronie, O., Seguini, L., Manfron, G., Lopez-
1153 Lozano, R., Baruth, B., Berg, M., Dentener, F., Ceglar, A., Chatzopoulos, T., and Zampieri, M.: The Exceptional 2018
1154 European Water Seesaw Calls for Action on Adaptation, *Earth’s Future* 7, 652–663,
1155 <https://doi.org/10.1029/2019EF001170>, 2019a.
- 1156 Toreti, A., Cronie, O. & Zampieri, M. Concurrent climate extremes in the key wheat producing regions of the world, *Sci. Rep.*,
1157 9, 5493, <https://doi.org/10.1038/s41598-019-41932-5> doi.org/10.1038/s41598-019-41932-5, 2019b.
- 1158 UNFCCC: Loss and Damage, online guide, United Nations Framework Convention on Climate Change, 46 pages,
1159 https://unfccc.int/sites/default/files/resource/loss_and_damage_online_guide.pdf, 2024~~1~~ (Accessed 19~~0~~ ~~October~~July
1160 2024~~3~~).
- 1161 van Delden, A.: The synoptic setting of thunderstorms in western Europe, *Atmos. Res.*, 56, 89–110,
1162 [https://doi.org/10.1016/S0169-8095\(00\)00092-2](https://doi.org/10.1016/S0169-8095(00)00092-2), 2001.
- 1163 van der Wiel, K., Lenderink, G., and de Vries, H.: Physical storylines of future European drought events like 2018 based on
1164 ensemble climate modelling, *Weath. Clim. Extremes*, 33, 100350, <https://doi.org/10.1016/j.wace.2021.100350>, 2021.
- 1165 Van Loon, A. F., and Van Lanen, H. A. J.: A process-based typology of hydrological drought. *Hydrol. Earth Syst. Sci.*, 16,
1166 1915–1946, <https://doi.org/10.5194/hess-16-1915-2012>, 2012.
- 1167 Vautard, R., van Oldenborgh, G. J., Otto, F. E. L., Yiou, P., de Vries, H., van Meijgaard, E., Stepek, A., Soubeyroux, J.-M.,
1168 Philip, S., Kew, S. F., Costella, C., Singh, R., and Tebaldi, C.: Human influence on European winter wind storms such as
1169 those of January 2018, *Earth Syst. Dynam.*, 10, 271–286, <https://doi.org/10.5194/esd-10-271-2019>, 2019.
- 1170 Vicente-Serrano, S. M., Beguería, S., and López-Moreno, J.I.: A Multiscalar Drought Index Sensitive to Global Warming: The
1171 Standardized Precipitation Evapotranspiration Index, *J. Climate*, 23, 1696–1718, <https://doi.org/10.1175/2009JCLI2909.1>,
1172 2010.

- 1173 Vogel, M. M., Zscheischler, J., Wartenburger, R., Dee, D., and Seneviratne, S. I.: Concurrent 2018 hot extremes across
1174 Northern Hemisphere due to human-induced climate change, *Earth's future*, 7, 692– 703,
1175 <https://doi.org/10.1029/2019EF001189>, 2019.
- 1176 von Bloh, W., Schaphoff, S., Müller, C., Rolinski, S., Waha, K., and Zaehle, S.: Implementing the nitrogen cycle into the
1177 dynamic global vegetation, hydrology, and crop growth model LPJmL (version 5.0), *Geosci. Model Develop.*, 11, 2789–
1178 2812. <https://doi.org/10.5194/gmd-11-2789-2018>, 2018.
- 1179 Wetter3.de (n.d.): Die ganze Welt in Wetterkarte. Retrieved 5 December 2022, from https://www.wetter3.de/index_dt.html
- 1180 Wild, M.: Global dimming and brightening: A review, *J. Geophys. Res.*, 114, D00D16, <https://doi.org/10.1029/2008JD011470>,
1181 2009.
- 1182 Wild, M.: Decadal changes in radiative fluxes at land and ocean surfaces and their relevance for global warming, *Wiley*
1183 *Interdisc. Reviews: Climate Change*, 7, 91-107, 2016.
- 1184 Yang, J., and Tian, H.: ISIMIP3b N-deposition input data (v1.0). ISIMIP Repository. <https://doi.org/10.48364/ISIMIP.600567>,
1185 2020.
- 1186 Zaitchik, B.F., Omumbo, J., Lowe, R., van Aalst, M., Anderson, L.O., Fischer, E., Norman, C., Robbins, J., Barciela, R.,
1187 Trtanj, J., von Borries, R., and Luterbacher, J.: Planning for compound hazards during the COVID-19 pandemic: the role
1188 of climate information systems. *Bull. Americ Meteorol. Soc.*, 103, E704-E709, 2022.
- 1189 Zampieri, M., Ceglar, A., Dentener, F., and Toreti, A.: Wheat yield loss attributable to heat waves, drought and water excess
1190 at the global, national and subnational scales, *Environ. Res. Lett.* 12, 064008. <https://doi.org/10.1088/1748-9326/aa723b>,
1191 2017.
- 1192 Zscheischler, J., and Fischer, E.M.: The record-breaking compound hot and dry 2018 growing season in Germany, *Weather*
1193 *Clim. Extrem.*, 29, 100270. <https://doi.org/10.1016/j.wace.2020.100270>, 2020.
- 1194 Zscheischler, J., Martius, O., Westra, S., Bevacqua, E., Raymond, C., Horton, R. M., van den Hurk, B., AghaKouchak, A.,
1195 Jézéquel, A., Mahecha, M. D., Maraun, D., Ramos, A. M., Ridder, N. N., Thiery, W. and Vignotto, E.: A typology of
1196 compound weather and climate events, *Nat. Rev. Earth Environ.*, 1, 333–347, <https://doi.org/10.1038/s43017-020-0060-z>,
1197 2020.
- 1198 Zscheischler, J. and Seneviratne, S.I.: Dependence of drivers affects risks associated with compound events, *Sci. Adv.* 3,
1199 e1700263, 2017.

